Stem Cell Reports
Article

ISSCR

OPEN ACCESS

Cell-Surface Protein Profiling Identifies Distinctive Markers of Progenitor Cells in Human Skeletal Muscle

Akiyoshi Uezumi,[1,*] Masashi Nakatani,[1] Madoka Ikemoto-Uezumi,[2] Naoki Yamamoto,[3] Mitsuhiro Morita,[4] Asami Yamaguchi,[4] Harumoto Yamada,[4] Takehiro Kasai,[5] Satoru Masuda,[6] Asako Narita,[6] Yuko Miyagoe-Suzuki,[6] Shin'ichi Takeda,[6] So-ichiro Fukada,[7] Ichizo Nishino,[8] and Kunihiro Tsuchida[1]

[1]Division for Therapies Against Intractable Diseases, Institute for Comprehensive Medical Science, Fujita Health University, 1-98 Dengakugakubo, Kutsukake, Toyoake, Aichi 470-1192, Japan
[2]Department of Regenerative Medicine, National Institute for Longevity Sciences, National Center for Geriatrics and Gerontology, 35 Gengo, Morioka, Obu, Aichi 474-8511, Japan
[3]Laboratory of Molecular Biology & Histochemistry
[4]Department of Orthopaedic Surgery
Fujita Health University, Toyoake, Aichi 470-1192, Japan
[5]Department of Orthopedic Surgery, Nagoya University Graduate School of Medicine, 65 Tsurumai, Showa-ku, Nagoya, Aichi 466-8550, Japan
[6]Department of Molecular Therapy, National Institute of Neuroscience, National Center of Neurology and Psychiatry (NCNP), 4-1-1 Ogawa-higashi, Kodaira, Tokyo 187-8502, Japan
[7]Department of Immunology, Graduate School of Pharmaceutical Sciences, Osaka University, 1-6 Yamada-oka, Suita, Osaka 565-0871, Japan
[8]Department of Neuromuscular Research, National Institute of Neuroscience, National Center of Neurology and Psychiatry (NCNP), 4-1-1 Ogawa-higashi, Kodaira, Tokyo 187-8502, Japan
*Correspondence: uezumi@fujita-hu.ac.jp
http://dx.doi.org/10.1016/j.stemcr.2016.07.004

SUMMARY

Skeletal muscle contains two distinct stem/progenitor populations. One is the satellite cell, which acts as a muscle stem cell, and the other is the mesenchymal progenitor, which contributes to muscle pathogeneses such as fat infiltration and fibrosis. Detailed and accurate characterization of these progenitors in humans remains elusive. Here, we performed comprehensive cell-surface protein profiling of the two progenitor populations residing in human skeletal muscle and identified three previously unrecognized markers: CD82 and CD318 for satellite cells and CD201 for mesenchymal progenitors. These markers distinguish myogenic and mesenchymal progenitors, and enable efficient isolation of the two types of progenitors. Functional study revealed that CD82 ensures expansion and preservation of myogenic progenitors by suppressing excessive differentiation, and CD201 signaling favors adipogenesis of mesenchymal progenitors. Thus, cell-surface proteins identified here are not only useful markers but also functionally important molecules, and provide valuable insight into human muscle biology and diseases.

INTRODUCTION

Skeletal muscle is an organ responsible for movement or physical activity, and therefore is vital for healthy life. Skeletal muscle is mainly composed of multinucleated cylindrical myofibers. Myofibers are terminally differentiated cells, and the cell cycle of their nuclei is irreversibly arrested. However, skeletal muscle regenerates well if myofibers are damaged and undergo necrosis. Skeletal muscle regeneration is attributable to the function of satellite cells that reside between the basal lamina and plasma membrane of myofibers. Satellite cells are normally quiescent, but rapidly become activated after muscle damage and proliferate extensively to produce myoblasts. Myoblasts then differentiate and fuse with each other or damaged myofibers to regenerate muscle. Some myoblasts remain undifferentiated and return to the quiescent state to maintain the satellite cell pool. Thus, satellite cells play a central role in muscle regeneration by acting as muscle stem cells (Bischof, 2004).

Skeletal muscle is also a site where pathological development of ectopic tissues occurs. Adipose tissue, fibrous connective tissue, or even bone can be ectopically formed within muscle not only in muscular disorders but also in other pathological conditions (Uezumi et al., 2014b). Because myofibers are terminally differentiated cells, they cannot be the source of these ectopic tissues. Hence, how these ectopic tissues emerge from skeletal muscle was a long-standing mystery. The identification of mesenchymal progenitors solved this mystery. We and others have identified mesenchymal progenitors distinct from satellite cells in mouse skeletal muscle and have shown that these mesenchymal progenitors contribute to ectopic adipose tissue (Joe et al., 2010; Uezumi et al., 2010), fibrous connective tissue (Uezumi et al., 2011), and heterotopic ossification (Wosczyna et al., 2012). Therefore, satellite cells and mesenchymal progenitors are indispensable cell types for studying skeletal muscle regeneration and pathogenesis, respectively.

Given that satellite cells and mesenchymal progenitors are strongly associated with muscle regeneration and pathogenesis, identifying, distinguishing, and isolating these two progenitor populations in human skeletal muscle are of considerable clinical significance. Compared with

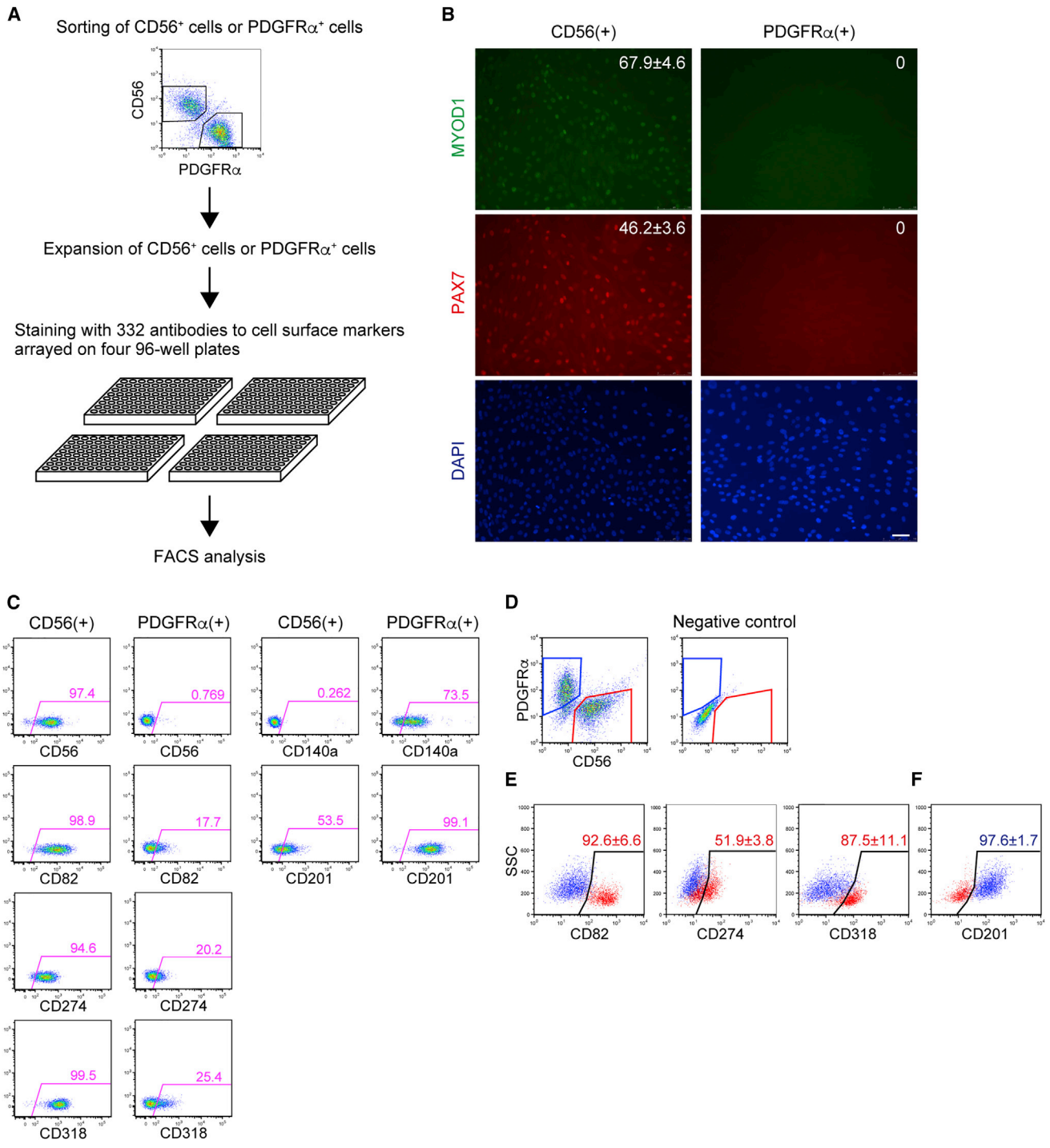

Figure 1. Cell-Surface Protein Profiling of Human Skeletal Muscle-Derived Progenitors by Antibody Screening

(A) Scheme of antibody screening.

(B) Expanded CD56$^+$ cells and PDGFRα$^+$ cells were stained with antibodies against MYOD1 and PAX7. The percentages of positive cells are shown in the panels as means ± SD, n = 5 randomly selected fields. Scale bar, 50 μm.

(C) Distinctive markers identified by antibody screening.

(D) Primary human skeletal muscle-derived cells were stained with antibodies against CD56, PDGFRα, and a newly identified marker. CD56$^+$ (red) and PDGFRα$^+$ (blue) gates were set by analyzing negative control samples stained with an isotype control antibody or secondary reagent only.

(legend continued on next page)

mouse, studies dealing with progenitor cells of human skeletal muscle are limited. In human satellite cells, only Pax7, M-cadherin, integrin α7, and CD56 have been considered to be specific markers (Boldrin et al., 2010; Castiglioni et al., 2014). Although Pax7 is a reliable marker for satellite cells in both mouse and human tissues (Boldrin and Morgan, 2012), this marker is not suitable for cell isolation because of its nuclear localization. M-cadherin has been reported to successfully identify human satellite cells (Boldrin and Morgan, 2012; Reimann et al., 2004; Sajko et al., 2004). We also identified satellite cells on human muscle sections using M-cadherin antibody (Uezumi et al., 2014a), but this antibody cannot be used for isolation of human myogenic cells. CD56 is the only marker that enables isolation of human satellite or myogenic cells, as distinguished from mesenchymal progenitors with adipogenic potential, known so far (Agley et al., 2013; Castiglioni et al., 2014; Uezumi et al., 2014a). Several markers have been reported to identify mesenchymal progenitors in human skeletal muscle. CD15 (Lecourt et al., 2010; Pisani et al., 2010a) and CD34 (Pisani et al., 2010b; Vauchez et al., 2009) were used to isolate cells with adipogenic potential, but adipogenic cells were also found in $CD15^-$ or $CD34^-$ populations of human muscle-derived cells (Agley et al., 2013; Castiglioni et al., 2014). A recent study reported the isolation of a mesenchymal stem cell-like population from human muscle-derived cells as $CD73^+CD105^+CD90^-$ cells (Downey et al., 2015). However, this study did not investigate myogenic cells; thus, whether these markers can isolate mesenchymal cells separately from myogenic satellite cells remains unclear. We know only platelet-derived growth factor receptor α (PDGFRα) as a marker that has been successfully used to isolate mesenchymal progenitors as being distinct from myogenic satellite cells from human skeletal muscle (Arrighi et al., 2015; Uezumi et al., 2014a).

To gain further insight into progenitor cells derived from human skeletal muscle, we performed comprehensive cell-surface protein profiling of two progenitor populations, $CD56^+$ myogenic progenitors and $PDGFR\alpha^+$ mesenchymal progenitors. This comprehensive analysis identified previously unrecognized markers: CD82 and CD318 for satellite cells and CD201 for mesenchymal progenitors. Immunofluorescent staining revealed that CD82 and CD318 are expressed on sublaminar satellite cells, and CD201 is expressed on interstitial mesenchymal progenitors in vivo. Isolated $CD82^+$ or $CD318^+$ cells showed high myogenic potential, while adipogenic potential was enriched exclusively in the $CD201^+$ population. Finally, CD82 knockdown resulted in premature differentiation at the expense of expansion and self-renewal of myogenic progenitors, and stimulation of CD201 signaling facilitated adipogenic differentiation of mesenchymal progenitors. Therefore, cell-surface proteins identified in this study are not only useful markers for cell identification and isolation but also functionally important molecules that regulate myogenesis and adipogenesis of human satellite cells and mesenchymal progenitors, respectively.

RESULTS

Cell-Surface Protein Profiling of Human Skeletal Muscle-Derived Progenitors by Antibody Screening

We previously reported the isolation of myogenic and mesenchymal progenitors from human skeletal muscle as $CD56^+$ and $PDGFR\alpha^+$ cells, respectively, and showed that physiological oxygen concentration has significant impact on growth of cells derived from human muscle (Uezumi et al., 2014a). We further optimized culture conditions for efficient expansion of isolated cells and found that collagen I coating and basic fibroblast growth factor (bFGF) promote proliferation of human muscle-derived progenitors (Figure S1). This condition allowed these progenitors to expand in vitro to 1×10^8 cells, which in turn enabled us to perform cell-surface protein profiling by antibody array. This analysis is based on the staining of cell-surface proteins with 332 antibodies and subsequent fluorescence-activated cell sorting (FACS) analysis (Figure 1A). We confirmed that expanded $CD56^+$ cells maintained the myogenic progenitor state, as revealed by PAX7 and myogenic differentiation 1 (MYOD1) positivity, and their surface phenotype as $CD56^+PDGFR\alpha^-$ (Figures 1B and 1C). On the other hand, $PDGFR\alpha^+$ cells maintained their non-myogenic nature and surface phenotype as $CD56^-PDGFR\alpha^+$ cells (Figures 1B and 1C). The entire dataset of $CD56^+$ cells and $PDGFR\alpha^+$ cells is shown in Figures S2 and S3, respectively. We first looked at previously reported markers that were used to isolate myogenic or mesenchymal progenitors from human

(E) Expressions of indicated markers on $CD56^+$ cells were analyzed. The $CD56^+$ population is shown in red. Positive gates were set by using $PDGFR\alpha^+$ cells as the negative population (blue). The percentages of positive cells in the $CD56^+$ population are shown in the panels as means ± SD, n = 13 for CD82, n = 4 for CD271, and n = 15 for CD318.

(F) Expression of CD201 on $PDGFR\alpha^+$ cells was analyzed. The $PDGFR\alpha^+$ population is shown in blue. A positive gate was set by using $CD56^+$ cells as the negative population (red). The percentage of positive cells in the $PDGFR\alpha^+$ population is shown in the panel as means ± SD, n = 6.

See also Figures S1–S4.

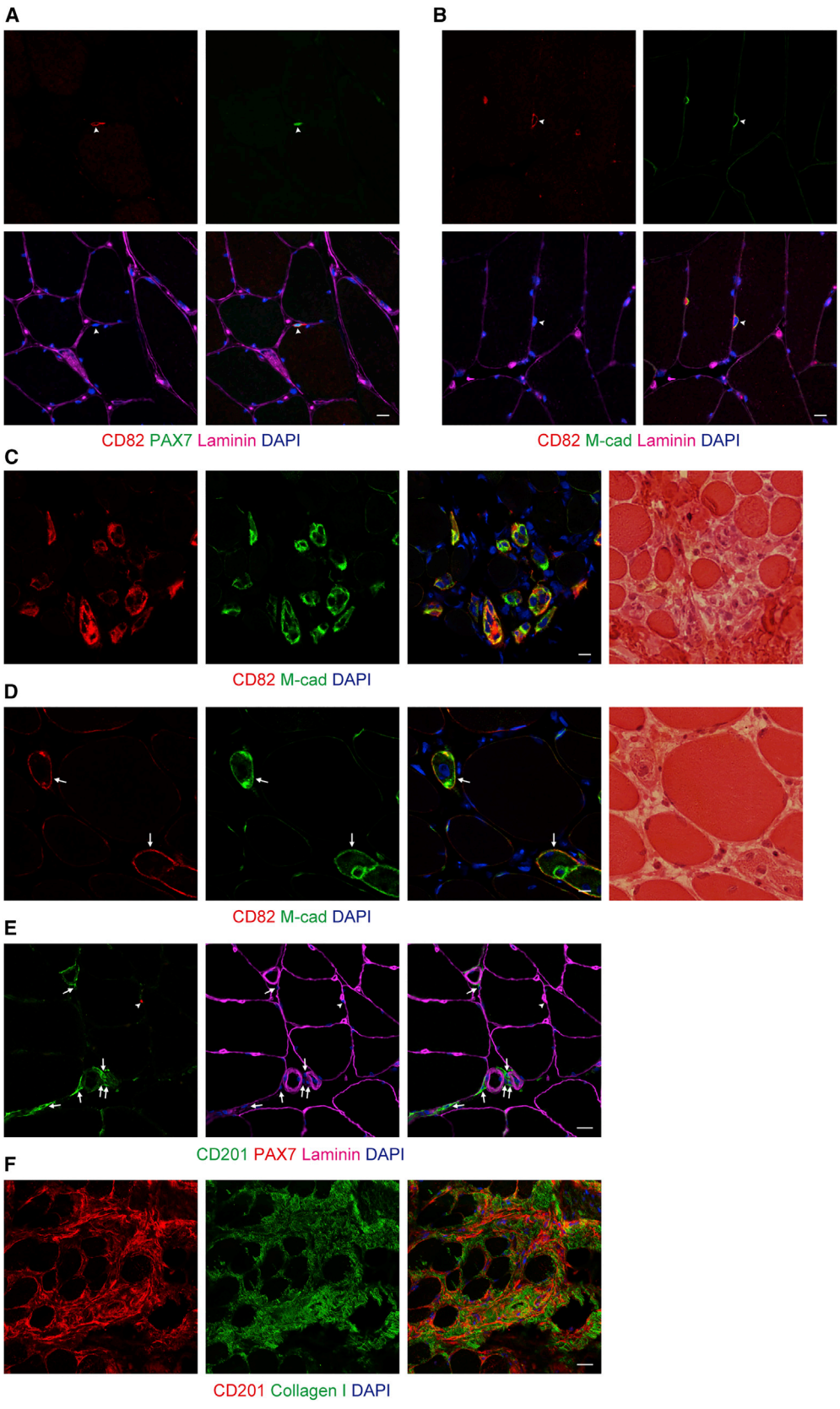

(legend on next page)

muscle. Charville et al. (2015) recently reported the isolation of human satellite cells using epidermal growth factor receptor (EGFR) as a marker, but we found that EGFR is expressed in both cultured myogenic and mesenchymal progenitors (Figures S2 and S3). Immunofluorescent staining of human muscle revealed that EGFR is indeed expressed by satellite cells but is also expressed by many interstitial cells (Figure S4A). Furthermore, interstitial PDGFRα$^+$ mesenchymal progenitors do express EGFR (Figure S4B), indicating that this marker cannot distinguish satellite cells from mesenchymal progenitors. CD15 (Lecourt et al., 2010; Pisani et al., 2010a), CD34 (Pisani et al., 2010b; Vauchez et al., 2009), CD73 (Downey et al., 2015), CD90 (Downey et al., 2015), and CD105 (Downey et al., 2015) were used to isolate mesenchymal progenitors, but all of these markers were found to be distributed equally on both cultured myogenic and mesenchymal progenitors (Figures S2 and S3).

We then searched for markers that are expressed differentially between two types of progenitors, and found that CD82, CD274, and CD318 are selectively expressed on cultured myogenic progenitors while CD201 is preferentially expressed on cultured mesenchymal progenitors (Figure 1C). Next, we confirmed results of antibody screening by analyzing primary cells derived from human skeletal muscle. CD82 and CD318 clearly distinguished CD56$^+$ myogenic progenitors from PDGFRα$^+$ mesenchymal progenitors, and the opposite could be achieved by using CD201 (Figures 1D and 1E). Because expression of CD274 was too weak to discriminate the two progenitors, we omitted this marker in the subsequent experiments (Figures 1D and 1E).

Expression of CD82, CD318, and CD201 in Human Skeletal Muscle Tissue

In vivo expression of identified markers was examined by using human muscle sections. Membrane expression of CD82 was clearly observed on PAX7$^+$ or M-cadherin$^+$ satellite cells in normal human muscle (Figures 2A and 2B). CD82 expression was found in almost all satellite cells (97.2% ± 0.6%: mean ± SD, n = 3 different healthy subjects, total number of satellite cells examined = 205). CD82 was predominantly expressed by satellite cells in muscle tissue, although we observed a small number of interstitial cells expressing CD82 (data not shown). We next examined Duchenne muscular dystrophy (DMD) muscle sections to investigate the expression of CD82 on activated satellite cells in vivo. CD82 signals were well overlapped on M-cadherin$^+$ activated satellite cells and also on M-cadherin$^+$ centrally nucleated nascent myofibers in DMD muscles (Figures 2C and 2D). These results indicate that CD82 is expressed on human satellite cells and its expression lasts until the early differentiation phase, but disappears as myofibers mature. A similar expression pattern was observed when human muscle sections were stained with antibody against CD318 (Figures S4C and S4E), although the percentage of positive satellite cells was relatively low (74.6% ± 5.6%; mean ± SD, n = 3 different healthy subjects, total number of satellite cells examined = 253), and cytoplasmic expression was also pronounced. In contrast to CD82 and CD318, CD201 antibody clearly recognized interstitial cells as distinguished from sublaminar PAX7$^+$ satellite cells (Figure 2E). CD201$^+$ cells could be seen with high frequency around blood vessels (Figure 2E). When DMD muscle sections were stained with anti-CD201 antibody, a considerable accumulation of CD201$^+$ cells was conspicuous in the areas of fibrosis where aberrant accumulation of collagen was observed (Figure 2F).

Isolation of Human Myogenic and Mesenchymal Progenitors Using Discovered Markers

To determine the efficacy of identified markers for progenitor cell isolation, we stained human muscle-derived cells with antibodies against CD82, CD318, or CD201. Staining with these markers resulted in clear separation of positive and negative populations (Figure 3A). If cell sorting was performed on the basis of CD82 or CD318 expression, PAX7$^+$MYOD1$^+$ myogenic progenitors were found only in CD82$^+$ or CD318$^+$ fractions (Figures 3B and 3C). When they were induced to differentiate into myotubes, many myosin heavy chain (MyHC)$^+$ myotubes developed only from CD82$^+$ or CD318$^+$ cells (Figure 3D). We next examined adipogenic differentiation after cell sorting based on CD201 expression. We detected adipogenic activity exclusively in CD201$^+$ cells (Figure 3E). Isolated CD201$^+$ cells were uniformly positive for CD201 in the growth

Figure 2. Expression of Discovered Markers in Adult Human Skeletal Muscle and DMD Muscle

(A and B) Adult human muscle sections were stained with antibodies against CD82, PAX7, and laminin (A) or CD82, M-cadherin, and laminin (B). Arrowheads indicate satellite cells located beneath the basement membrane.

(C and D) DMD muscle sections were subjected to immunofluorescent staining for CD82 and M-cadherin, and subsequently to H&E staining. Arrows indicate centrally nucleated M-cadherin$^+$ myofibers.

(E) Adult human muscle sections were stained with antibodies against CD201, PAX7, and laminin. Arrows indicate CD201$^+$ cells located in interstitial spaces, and arrowheads indicate satellite cell located beneath the basement membrane.

(F) DMD muscle sections were stained with antibodies against CD201 and collagen I.

Scale bars represent 10 μm (A–D) and 20 μm (E and F). See also Figure S4.

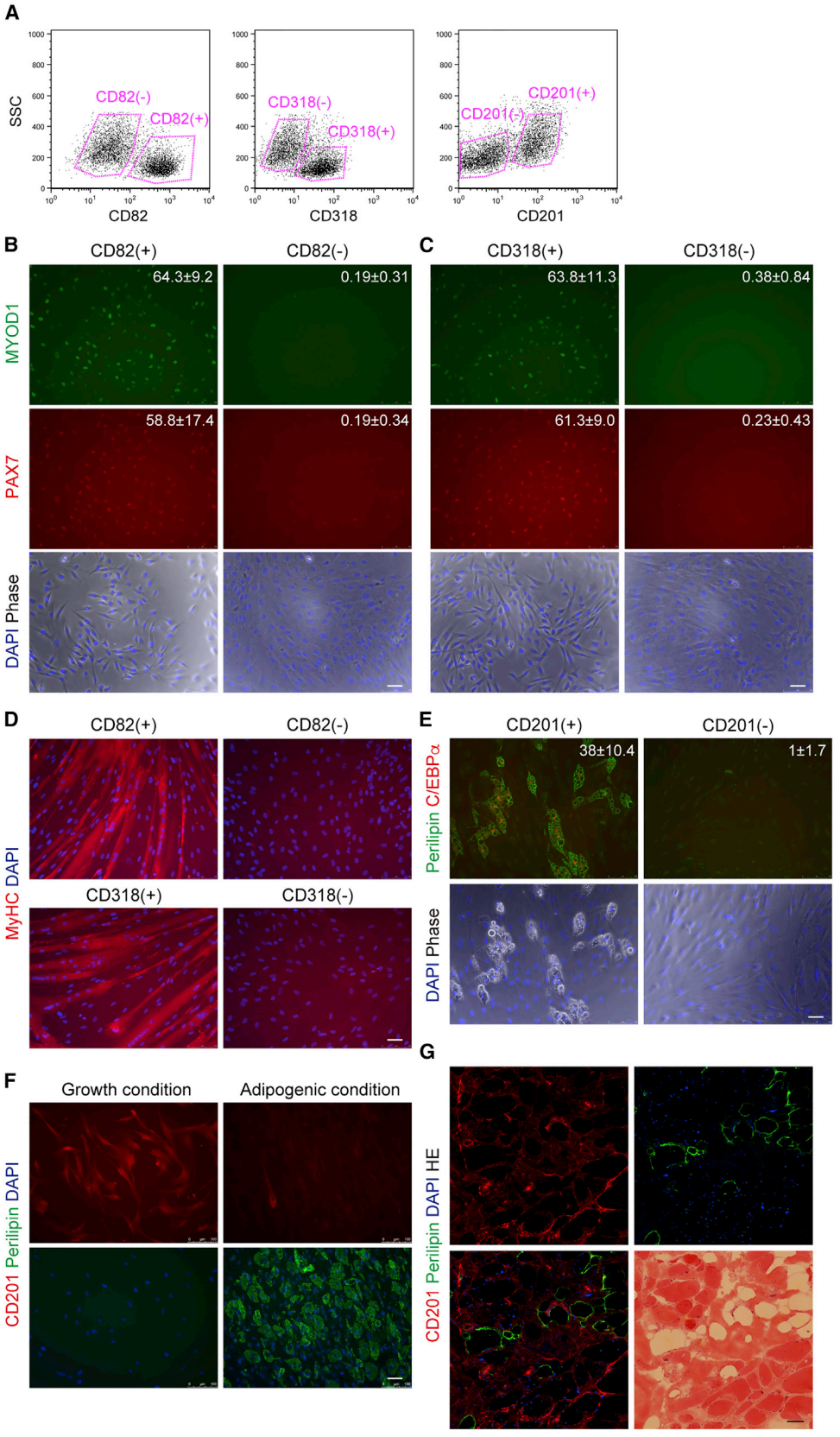

(legend on next page)

condition, but in the adipogenic condition, expression of CD201 disappeared from differentiated adipocytes and was maintained in only a few undifferentiated cells (Figure 3F). Likewise, ectopic adipocytes developed within skeletal muscle were also negative for CD201 (Figure 3G), suggesting a link between expression of CD201 and the undifferentiated state. These results indicate that markers identified by cell-surface protein profiling are useful for efficient isolation of progenitor cells from human muscle. We also examined the expression of identified markers in commercially available human skeletal muscle myoblast (HSMM) cultures. $CD56^+$ cells were strongly positive for CD82, but expression of CD318 was reduced in HSMM cultures (Figure S5A). When cell sorting was done on the basis of CD56 and CD82 expression, myogenic cells were exclusively found in the $CD56^+CD82^+$ fraction (Figures S5B–S5D). Surprisingly, many $PDGFR\alpha^+$ non-myogenic cells were present in HSMM cultures and were positive for CD201 (Figure S5E). Adipogenic potential was detected only in this $PDGFR\alpha^+CD201^+$ fraction (Figure S5F). Thus, markers described here are also useful in the purification of progenitor cells from commercially available cultures. These results prompted us to use discovered makers for purifying myogenic progenitors from human induced pluripotent stem cells (iPSCs). Human iPSCs (clone 253G4) (Nakagawa et al., 2008) were induced to differentiate into myogenic cells as previously described (Figure S6A) (Hosoyama et al., 2014), and the induced cells were examined for expression of CD82 and CD318. Although CD318 was not detected, a $CD82^+$ fraction was readily identified in iPSC-derived cells (Figure S6B) and $CD82^+$ cells showed considerably high expression of myogenic progenitor-related genes compared with other fractions (Figure S6C), indicating that myogenic progenitors are exclusively enriched in the $CD82^+$ fraction of human iPSC-derived cells. Similar results were obtained when another iPSC line (clone 201B7) (Takahashi et al., 2007) was used (Figure S6D). To further explore the usefulness of CD82 as a myogenic marker, we divided iPSCs (clone 454E2) (Okita et al., 2011) induced to a myogenic lineage into four fractions based on the expression of CD82 and CD56 (Figure S6E). After cell sorting, we found that myotube forming activity was highly enriched in $CD82^+CD56^+$ cells (Figure S6F). Thus, CD82 is a useful myogenic marker that is applicable to the isolation of myogenic progenitors not only from human skeletal muscle but also from human iPSCs.

In Vivo Myogenic Potential of $CD82^+$ Cells or $CD318^+$ Cells, and Fibrogenic/Adipogenic Potential of $CD201^+$ Cells

The in vivo myogenic potential of $CD82^+$ or $CD318^+$ cells isolated from human muscle was evaluated by transplantation into injured muscles of immunodeficient mice. Fifteen days after transplantation, many human $spectrin^+$ myofibers that contain human $lamin^+$ nuclei were observed in the muscles that had received $CD82^+$ or $CD318^+$ cells (Figures 4A and 4B; Table 1). In addition to differentiated myofibers, occasional human $Lamin^+$ and $PAX7^+$ sublaminar satellite cells could be detected in $CD82^+$ or $CD318^+$ cell-transplanted muscles (Figure 4C and Table 1), indicating that transplanted $CD82^+$ or $CD318^+$ cells possess self-renewal potential. Such in vivo myogenic activity was detected in all $CD82^+$ or $CD318^+$ populations prepared from four independent samples, but rarely seen in $CD82^-$ or $CD318^-$ cells (Table 1). To evaluate in vivo differentiation potential of $CD201^+$ cells, we permanently labeled $CD201^+$ cells with the fluorescent protein Venus by using lentiviral vector. We confirmed that $CD201^+$ cells were efficiently transduced with Venus (Figure 4D), and Venus labeling did not affect adipogenic differentiation (Figure 4E). After sorting of Venus-labeled $CD201^+$ cells, the cells were transplanted into glycerol-injured muscles of immunodeficient mice. Two weeks after transplantation, many $Venus^+$ cells were detected in fatty/fibrous degenerated areas and some of them expressed peroxisome proliferator-activated

Figure 3. Efficient Isolation of Myogenic Progenitors by CD82 or CD318 and Mesenchymal Progenitors by CD201

(A) Primary human skeletal muscle-derived cells were stained with antibodies against indicated markers and divided into positive and negative fractions. Sorting gates are shown in the panels.

(B and C) The indicated cell populations were cultured in the growth condition for 3 days and then stained with antibodies against MYOD1 and PAX7. The percentages of positive cells are shown in the panels as means ± SD, n = 15 fields from three independent preparations.

(D) The indicated cell populations were cultured in the myogenic differentiation condition for 5 days and then stained with antibody against myosin heavy chain (MyHC).

(E) The indicated cell populations were cultured in the growth condition for 3 days, then cells were subjected to the adipogenic condition. Cells were stained with antibodies against perilipin and C/EBPα. Numbers of adipocytes per field are shown in the panels as means ± SD, n = 15 fields from three independent preparations.

(F) $CD201^+$ cells grown in growth condition or subjected to the adipogenic condition were stained with antibodies against CD201 and perilipin.

(G) Human muscle samples with ectopic adipocytes were subjected to immunofluorescent staining for CD201 and perilipin, and subsequently to H&E staining.

Scale bars, 50 μm. See also Figures S5 and S6.

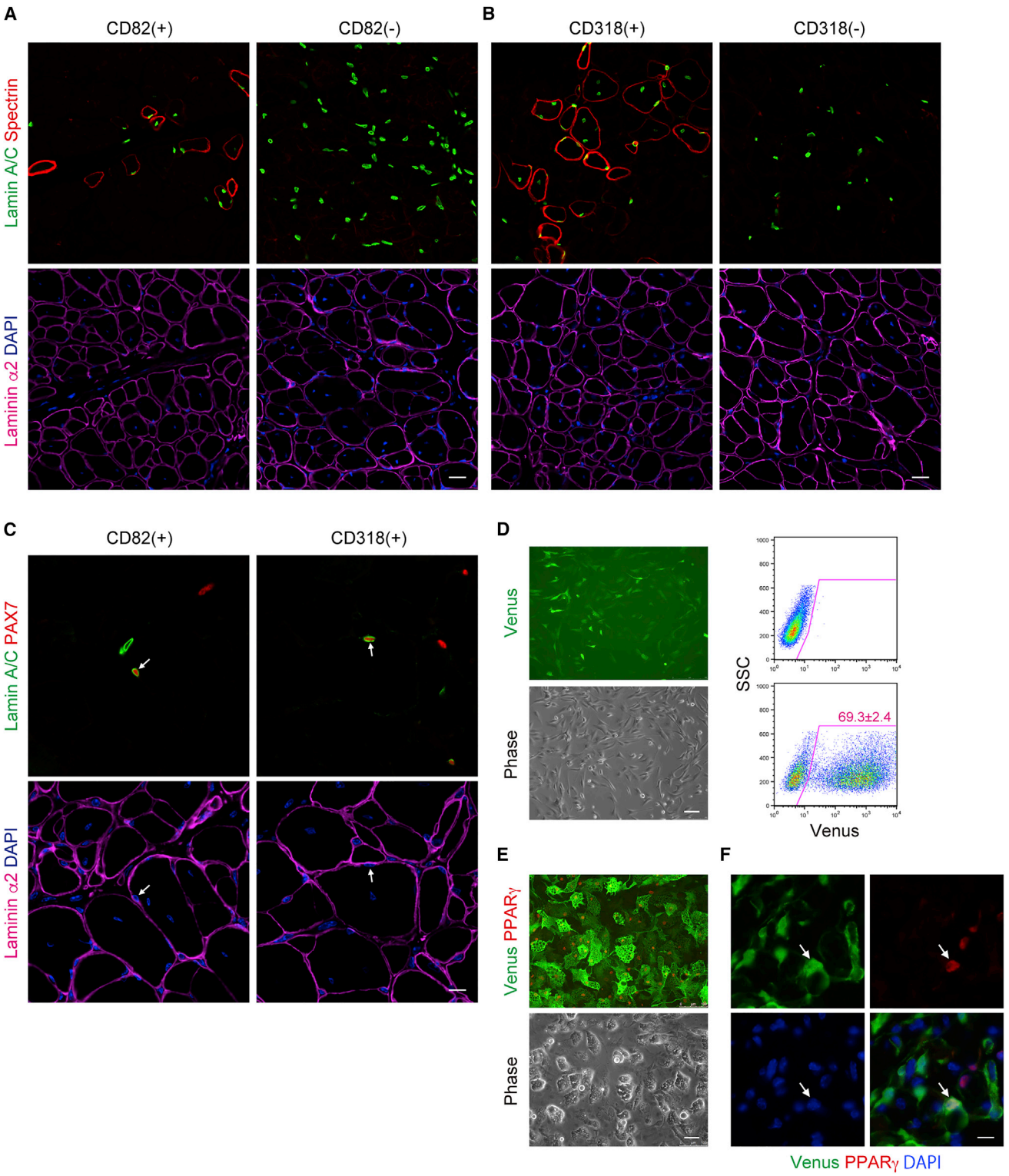

Figure 4. In Vivo Myogenic Potential of CD82$^+$ Cells or CD318$^+$ Cells, and Fibrogenic/Adipogenic Potential of CD201$^+$ Cells

(A–C) The indicated cell populations were transplanted into CTX-injured muscles of immunodeficient mice. Transplanted muscle sections were subjected to immunofluorescent staining for human lamin A/C, human spectrin, and laminin α2 (A, B), or human lamin A/C, PAX7, and laminin α2 (C). Arrows indicate lamin A/C$^+$PAX7$^+$ human satellite cells located beneath the basement membrane.

(legend continued on next page)

Table 1. Summary of Transplantation Experiment

Patient	Cell Type	Number of Transplanted Cells	Number of Lamin A/C$^+$ Cells/Section	Number of Spectrin$^+$ Myofibers/Section	Number of Lamin A/C$^+$PAX7$^+$ Cells/Section
Hu36	CD82$^+$	8×10^4	45	23	0
	CD82$^+$	8×10^4	20	10	3
	CD82$^+$	8×10^4	35	20	3
	CD82$^-$	5×10^4	90	2	0
	CD318$^+$	7×10^4	125	70	9
	CD318$^+$	7×10^4	50	28	7
	CD318$^+$	7×10^4	61	25	3
	CD318$^-$	5×10^4	66	0	0
Hu37	CD82$^+$	6×10^4	70	16	0
	CD82$^+$	6×10^4	57	13	1
	CD82$^-$	6×10^4	352	0	0
	CD82$^-$	6×10^4	109	0	0
	CD82$^-$	6×10^4	220	0	0
Hu38	CD82$^+$	1×10^5	12	7	1
	CD82$^+$	1×10^5	12	3	0
	CD82$^-$	1×10^5	26	0	0
	CD82$^-$	1×10^5	15	0	0
Hu39	CD318$^+$	1×10^5	55	14	2
	CD318$^+$	1×10^5	35	15	1
	CD318$^-$	1×10^5	179	1	0
	CD318$^-$	1×10^5	19	0	0

receptor γ (PPARγ) (Figure 4F), suggesting the functional importance of these cells in muscle pathogenesis.

Function of CD82 and CD201 in Human Myogenic and Mesenchymal Progenitors

We explored roles of discovered markers in the regulation of progenitor function. Because CD82 is consistently expressed myogenic cells from human muscle, commercially available cells, and iPSCs, we knocked down CD82 in CD56$^+$CD82$^+$ myogenic cells purified from human muscle by small interfering RNA (siRNA). Almost complete knockdown of CD82 was confirmed at both mRNA and protein levels (Figure 5A). Intriguingly, knocked-down CD82 cells showed reduced proliferation and increased *MYOD1* and *MYOG* transcript level even under growth condition (Figures 5B and 5C). Although the percentage of MYOD1$^+$ cells remained unchanged, the percentage of myogenin (MYOG)$^+$ cells and the total amount of MYOD1 and MYOG protein were dramatically increased in knocked-down CD82 cells (Figures 5D–5F), indicating that CD82 knockdown leads to premature differentiation. Because p38 signaling is well known to be involved in myogenic differentiation, we examined this signaling pathway. Phosphorylation of p38 was increased upon CD82 knockdown

(D) CD201$^+$ cells transduced with Venus were analyzed by fluorescent microscope and FACS.
(E) Venus-labeled CD201$^+$ cells were stained with antibodies against GFP and PPARγ.
(F) Venus-labeled CD201$^+$ cells were transplanted into glycerol-injured muscles of immunodeficient mice. Transplanted muscle sections were stained with antibodies against GFP and PPARγ. Arrow indicates Venus$^+$ adipocyte expressing PPARγ.
Scale bars represent 20 μm (A and B), 10 μm (C and F), 100 μm (D), and 50 μm (E).

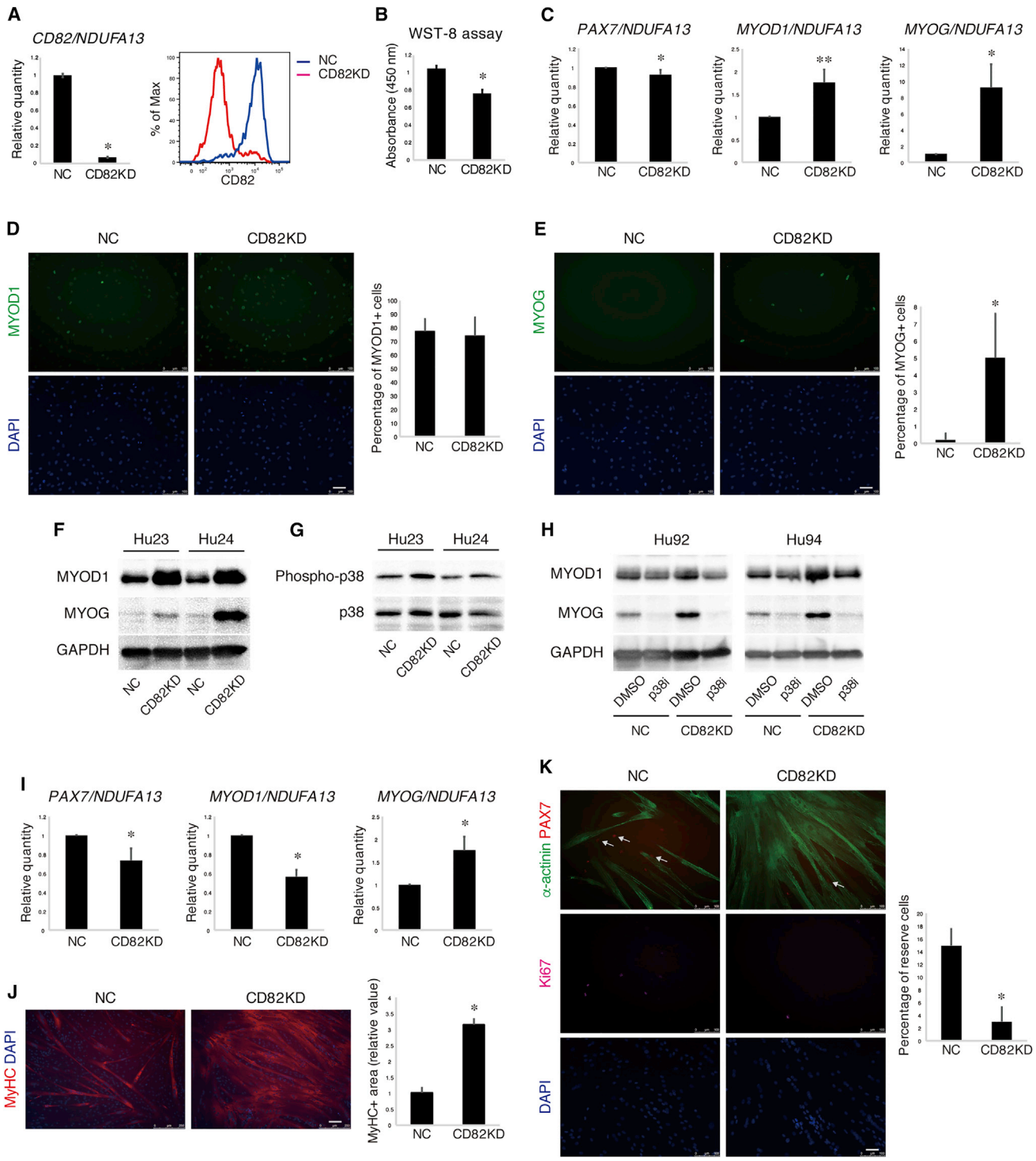

Figure 5. Knockdown of CD82 Leads to Premature Differentiation in Myogenic Progenitors at the Expense of Expansion and Reserve Cell Generation

(A) $CD56^{+}CD82^{+}$ cells were purified and cultured. Cells were transfected with negative control siRNA (NC) or CD82 siRNA (CD82KD). The indicated cells were cultured in the growth condition for 2 days. The expression of *CD82* mRNA was quantified by qRT-PCR. Values are represented as the ratio to control cells and shown as means ± SD of three independent preparations. *$p < 0.01$ (left). The expression of CD82 protein was measured by FACS (right).

(legend continued on next page)

(Figure 5G), and the excessive upregulation of MYOD1 and MYOG induced by CD82 knockdown was suppressed by p38 inhibitor (Figure 5H), suggesting that CD82 inhibits premature differentiation at least in part by attenuating the p38 signaling pathway. When induced to differentiate into myotubes, knocked-down CD82 cells showed a significant decrease in the levels of *PAX7* and *MYOD1* transcript but maintained increased *MYOG* expression (Figure 5I). Knocked-down CD82 cells exhibited extravagant differentiation (Figure 5J) and reduced the number of reserve cells compared with control cells (Figure 5K). These results suggest that CD82 is required for achieving an appropriate balance between differentiation and self-renewal of human myogenic progenitors.

CD201 acts as a receptor for protein C (PC) and activated protein C (APC). CD201 forms a complex with PC and thrombomodulin (TM) to exert its major function, anticoagulation, but also initiates diverse intracellular signaling in the presence of co-receptor protease-activated receptor 1 (PAR1) upon APC binding (Mohan Rao et al., 2014). When analyzed by FACS, PAR1 was found to be expressed strongly on the surface of human mesenchymal progenitors, although only faint expression of TM was detected (Figure 6A), which suggests that mesenchymal progenitors can elicit signals through CD201-PAR1 receptors upon APC binding. To gain insight into the role of CD201 signaling in mesenchymal progenitors, we added APC to the medium during adipogenic differentiation. Although the total number of cells remained unchanged (data not shown), adipocyte formation was significantly enhanced in the presence of APC (Figures 6B and 6C). However, mesenchymal progenitors showed no adipogenesis when treated with the medium containing APC but not adipogenic-inducing reagents (Figure 6D), suggesting that CD201 signaling per se cannot initiate adipogenesis but reinforces the adipogenic program evoked by other inductive cues. Akt and Erk are important signaling pathways that enhance central the adipogenic program governed by PPARγ (Peng et al., 2003; Prusty et al., 2002). When treated with APC, both Akt and Erk pathways were activated in mesenchymal progenitors (Figure 6E). Our data suggest that CD201 signaling favors adipogenesis through activating Akt and Erk pathways in mesenchymal progenitors.

DISCUSSION

In this study, we comprehensively analyzed the cell-surface phenotype of two types of progenitor cells residing in human skeletal muscle. As a consequence, we identified three previously unknown cell-surface markers: CD82 and CD318 for myogenic progenitors and CD201 for mesenchymal progenitors. In human muscle tissue, sublaminar satellite cells express both CD82 and CD318, and interstitial mesenchymal progenitors express CD201. Intriguingly, these markers can distinguish between myogenic and mesenchymal progenitors, and are applicable to efficient isolation of the two types of progenitor cells. Considering the limited information about progenitor cells residing in human skeletal muscle, our comprehensive analysis provides profound insight into their characteristics by defining the cell-surface phenotype of myogenic progenitors as $CD56^{+}CD82^{+}CD318^{+}PDGFR\alpha^{-}CD201^{-}$ and that of mesenchymal progenitors as $CD56^{-}CD82^{-}CD318^{-}PDGFR\alpha^{+}CD201^{+}$.

CD82, also known as KAI1, is a member of the tetraspanin family. Although tetraspanins are involved in a wide variety of biological processes such as cell adhesion, migration, proliferation, and signal transduction (Liu and Zhang, 2006), CD82 is probably best known as a metastasis

(B) Cell proliferation was measured by using WST-8 reagent and shown as means ± SD of three independent preparations. *$p < 0.01$.
(C) The expressions of myogenic genes were quantified by qRT-PCR. Values are represented as the ratio to control cells and shown as means ± SD of four independent preparations. *$p < 0.01$, **$p < 0.05$.
(D and E) Cells were stained with antibodies against MYOD1 or MYOG. The percentages of positive cells are shown as means ± SD, n = 20 fields from four independent preparations. *$p < 0.01$
(F) Western blot analysis of MYOD1, MYOG, and GAPDH. Results from two independent preparations are shown.
(G) Phosphorylation of p38 was assessed by immunoblotting. Results from two independent preparations are shown.
(H) Control or knocked-down CD82 cells were treated with SB203580 (p38i) or DMSO. The expression of MYOD1, MYOG, and GAPDH was analyzed by immunoblotting. Results from two independent preparations are shown.
(I) After 2 days of culture in growth condition, cells were induced to differentiate into myotubes. The expressions of myogenic genes were quantified by qRT-PCR. Values are represented as the ratio to control cells and are shown as means ± SD of four independent preparations. *$p < 0.01$.
(J) The indicated cells were stained with antibody against MyHC and the $MyHC^{+}$ area was quantified. Values are represented as the ratio to control cells and are shown as means ± SD of three independent preparations. *$p < 0.01$.
(K) The indicated cells were stained with antibody against sarcomeric α-actinin, PAX7, and Ki67. Arrows indicate $PAX7^{+}Ki67^{-}$ undifferentiated reserve cells. The percentages of reserve cells are shown as means ± SD, n = 9 fields from three independent preparations. *$p < 0.01$.
Scale bars represent 50 μm (D, E, K) and 100 μm (J).

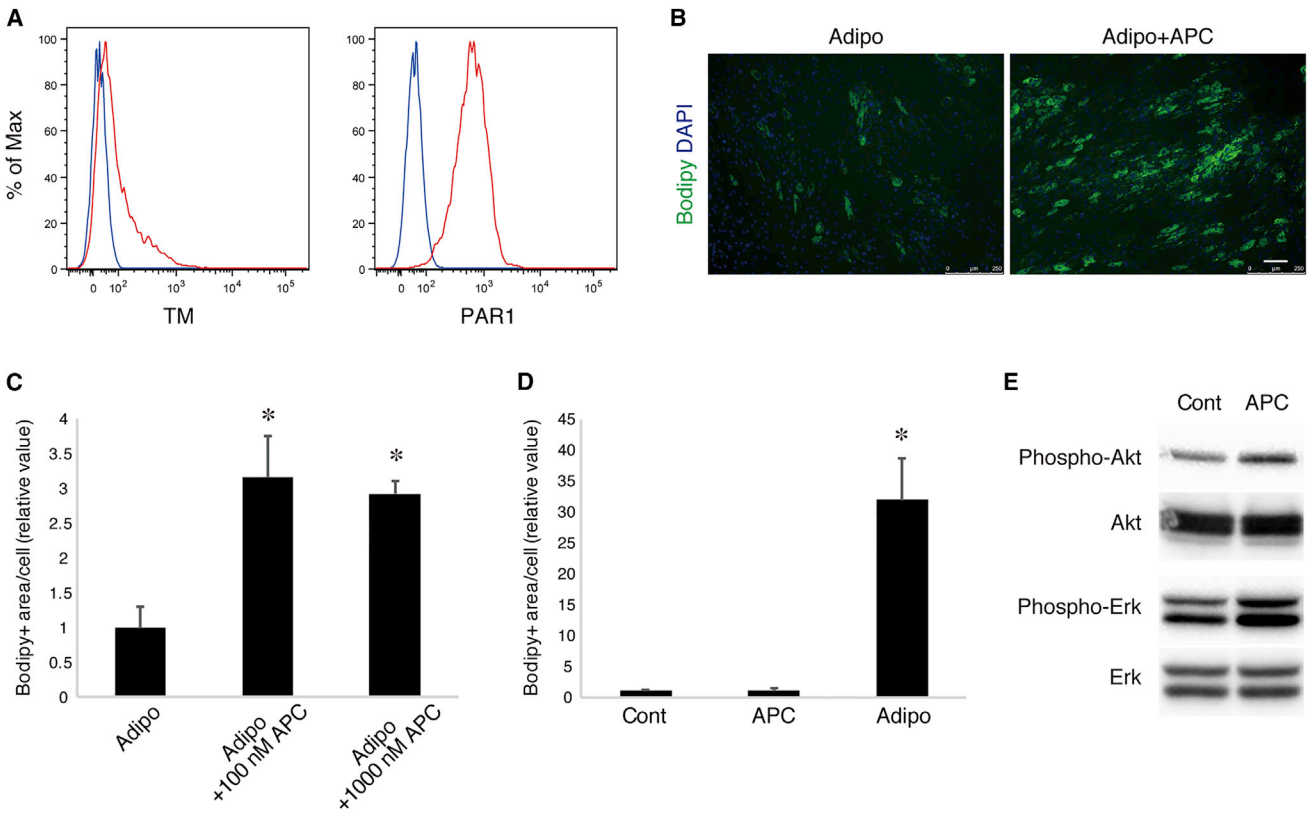

Figure 6. CD201 Signaling Facilitates Adipogenesis of Mesenchymal Progenitors

(A) The cell-surface expression of TM and PAR1 was analyzed by FACS. Isotype control is shown in blue and antibody-stained sample in red.

(B) Mesenchymal progenitors were induced to differentiate into adipocytes with (Adipo + APC) or without (Adipo) APC. Lipid droplets were stained with Bodipy.

(C) Adipocyte differentiation was quantified by measuring Bodipy^{+} area per cell. Values are represented as the ratio to cells not treated with APC and shown as means ± SD of three independent preparations. *$p < 0.01$.

(D) Mesenchymal progenitors were cultured in 10% FBS/DMEM (Cont), 10% FBS/DMEM supplemented with APC (APC), or adipogenic differentiation condition (Adipo). Adipocyte differentiation was quantified, and values are represented as the ratio to control cells and shown as means ± SD of three independent preparations. *$p < 0.01$.

(E) Mesenchymal progenitors were serum starved overnight and then stimulated with APC for 30 min. Phosphorylation of Akt and Erk were assessed by immunoblotting.

suppressor (Dong et al., 1995). Expression of CD82 was reported in many non-muscle tissues (Custer et al., 2006; Huang et al., 1997; Nagira et al., 1994), and low-level expression of CD82 was also detected in skeletal muscle (Custer et al., 2006; Nagira et al., 1994). However, the detailed expression pattern of CD82 in skeletal muscle has not been examined. In this study, we demonstrated that CD82 is expressed on satellite cells in normal human skeletal muscle and on activated satellite cells or small regenerating myofibers in DMD muscle, but is absent in mature myofibers. Expression of CD82 seems to be specific to immature myogenic cells in human skeletal muscle because only a few CD82^{+} cells could be seen in the interstitial spaces. Specific expression of CD82 in myogenic cells is further supported by a microarray study of mouse satellite cells (Fukada et al., 2007) that showed high-level expression of CD82 in satellite cells compared with non-myogenic cells (Table S1). Such specificity provides significant value as a marker, because other markers used for the isolation of human satellite cells such as CD29 and EGFR (Charville et al., 2015; Xu et al., 2015) are also expressed in non-myogenic cells. Knockdown experiments revealed that CD82 suppresses premature differentiation by inhibiting MYOD1 and MYOG expression in human myogenic progenitors. We further showed that knocked-down CD82 cells exhibited excessive differentiation at the expense of generation of reserve cells, which represent an in vitro model of self-renewal. Although CD82 has received scant attention in stem cell biology, recent study demonstrated an important role for this cell-surface molecule in

maintaining hematopoietic stem cell (HSC) quiescence (Hur et al., 2016), which is suggestive of a general role for CD82 in stem cell maintenance. Our data suggest that CD82 exerts its effects on myogenic progenitors through attenuating p38 signaling, although we cannot exclude other mechanisms that mediate CD82 functions. Precise mechanisms whereby CD82 suppresses MYOD1 and MYOG, and thereby ensures expansion and self-renewal of human myogenic progenitors, are of great interest.

CD318, also known as CUB domain-containing protein 1, acts as a substrate for Src family kinases and is associated with the metastatic potential of cancer cells (Wortmann et al., 2009). In addition to cancer cells, CD318 has been reported to be present in several stem/progenitor populations such as hematopoietic stem/progenitor cells, mesenchymal stem cells, and neural progenitor cells (Buhring et al., 2004; Conze et al., 2003; Takeda et al., 2010). We reported here that CD318 is also expressed on human myogenic progenitors with an expression pattern similar to that of CD82. However, expression of CD318 was diminished in commercially available myoblasts and undetectable in iPSC-derived cells. Although the exact reason for the downregulation of CD318 is currently unknown, the oxygen concentration used in those cultures differed from that in our culture condition. We used a hypoxic condition for cell culture, but commercially available myoblasts or iPSCs were cultured in a normoxic condition. Because expression of CD318 is induced by hypoxia (Cao et al., 2015; Emerling et al., 2013; Razorenova et al., 2011), a different oxygen concentration might lead to a difference in CD318 expression.

CD201, also known as endothelial protein C receptor, is a type 1 transmembrane glycoprotein expressed in the endothelium of large blood vessels and also in many other cell types (Mohan Rao et al., 2014). Its well-known function is anticoagulation. Our analysis revealed that CD201 is specifically expressed in mesenchymal progenitors but not in myogenic satellite cells within human skeletal muscle. While previously reported mesenchymal markers such as CD15 (Lecourt et al., 2010; Pisani et al., 2010a), CD34 (Pisani et al., 2010b; Vauchez et al., 2009), CD73 (Downey et al., 2015), CD90 (Downey et al., 2015), and CD105 (Downey et al., 2015) were distributed equally on both cultured myogenic and mesenchymal progenitors, our comprehensive analysis identifies one of the most powerful markers, which is equivalent to PDGFRα and can distinguish mesenchymal progenitors from myogenic cells. We also found that human mesenchymal progenitors highly express PAR1, a co-receptor of CD201. CD201 is selectively expressed in HSCs (Balazs et al., 2006), and CD201-PAR1 signaling has been recently shown to regulate the retention and recruitment of HSCs within the bone marrow microenvironment (Gur-Cohen et al., 2015). We showed in this study that stimulation of CD201-PAR1 signaling in mesenchymal progenitors leads to enhanced adipogenesis by activating the Akt and Erk pathway. Thus, our study further unveils an additional function of CD201, which is traditionally recognized as a coagulation-related factor, as a regulator of stem/progenitor cell function.

In conclusion, we identified previously unrecognized markers of two types of progenitor cells residing in human skeletal muscle by comprehensive cell-surface protein profiling. These markers are quite unique in being able to distinguish between myogenic and mesenchymal progenitors, and in regulating myogenesis and adipogenesis. Our study provides meaningful information not only for the basic science of human skeletal muscle but also for practical research, including regenerative medicine for muscle diseases.

EXPERIMENTAL PROCEDURES

Human Muscle Samples

Experiments using human samples were approved by the Ethical Review Board for Clinical Studies at Fujita Health University. Non-dystrophic muscle samples were obtained from gluteus medius muscles of subjects undergoing total hip arthroplasty. DMD muscle samples were obtained from muscle (rectus femoris or biceps brachii) biopsies performed for diagnostic purposes. A human myoblast culture was purchased from Lonza.

Dissociation of Cells from Muscle Samples

Muscles were transferred to PBS and digested with 0.2% type II collagenase (Worthington). Muscle slurries were filtered through a cell strainer (BD Biosciences). Cells were resuspended in growth medium (GM) consisting of DMEM supplemented with 20% fetal bovine serum (FBS), 1% penicillin-streptomycin, and 2.5 ng/mL bFGF (Katayama Chemical), seeded onto a collagen I-coated dish (Iwaki), and maintained at 37°C in 5% CO_2 and 3% O_2.

FACS

Cells were trypsinized and resuspended in washing buffer consisting of PBS with 2.5% FBS, and stained with primary antibodies. Cells were then stained with secondary reagents. Primary antibodies and secondary reagents used are described in Supplemental Experimental Procedures. Stained cells were analyzed by FACSVerse, FACSVantage SE (BD Biosciences), or MoFlo Astrios (Beckman Coulter). Cell sorting was performed on a FACSVantage SE or MoFlo Astrios.

Antibody Screening

After cell sorting, $CD56^+$ cells or $PDGFR\alpha^+$ cells were cultured in GM on a collagen I-coated dish at 37°C in 5% CO_2 and 3% O_2, and expanded to 1×10^8 cells. Antibody screening was carried out using a LEGENDScreen human cell screening kit (BioLegend).

Cell Culture

Sorted cells were cultured on Matrigel-coated (BD Biosciences) plates in GM at 37°C in 5% CO_2 and 3% O_2. Ten thousand cells were added per well. Myogenic and adipogenic differentiation were carried out as described in Supplemental Experimental Procedures. CD82 knockdown was performed by transfecting CD82 siRNA (Ambion). Cell proliferation was measured using Cell Counting Kit-8 (Dojindo). SB203580 (Wako), a p38 inhibitor, was used at 10 μM. APC (Haematologic Technologies) was used at 100 or 1,000 nM.

iPSCs and Induction of Myogenic Progenitors

Human iPSCs were provided by the Center for iPS Cell Research and Application. Myogenic cells were induced from iPSCs as previously described (Hosoyama et al., 2014). Induced cells were trypsinized and resuspended in washing buffer, then subjected to FACS sorting.

Generation of Lentiviral Vector and In Vitro Transduction

Plasmids required for generation of lentiviral vector were obtained from RIKEN BRC. The lentiviral vector was generated as described by Ikemoto et al. (2007). Sorted $CD201^+$ cells were infected with 200 MOI of viral vector.

Transplantation Experiment

All procedures using experimental animals were approved by the Institutional Animal Care and Use Committee at Fujita Health University. Immunodeficient NOD/scid or NSG mice were used. One day prior to transplantation, tibialis anterior (TA) muscles were injured with cardiotoxin (CTX) or glycerol as described by Uezumi et al. (2010). Cells in 25 μL of PBS were transplanted into injured TA muscles. Fifteen days after transplantation, TA muscles were sampled and subjected to histological analysis.

Histochemistry, Cytochemistry, and Microscopy

For CD82 and CD318 immunostaining, sections were treated with Antigen Retrieval Reagent-Universal solution (R&D Systems) at 95°C for 5 min. Specimens were blocked with protein-block serum-free reagent (Dako) for 15 min, and incubated with primary antibodies at 4°C overnight, followed by secondary staining. Antibodies used are described in Supplemental Experimental Procedures. Specimens were counterstained with DAPI (Invitrogen) and mounted with SlowFade Gold anti-fade reagent (Invitrogen). Stained samples were photographed using a fluorescence microscope BX51 (Olympus), an inverted fluorescence microscope BZ-9000 (Keyence), or an inverted fluorescence microscope DMI4000B (Leica). Confocal images of muscle sections were taken using the confocal laser scanning microscope system LSM700 (Carl Zeiss).

Immunoblotting

Cells were lysed in lysis buffer containing protease inhibitor cocktail (Roche). For the detection of phosphorylated proteins, phosphatase inhibitor cocktail (Roche) was added. Ten micrograms of protein was separated by SDS-PAGE and transferred onto polyvinylidene difluoride membranes. The membranes were probed with primary antibodies described in Supplemental Experimental Procedures. After incubation with horseradish peroxidase-conjugated secondary antibodies and chemiluminescence reactions, images of the developed immunoblots were captured using a Light-Capture imaging system (ATTO).

Quantitative Analyses of Cultured Cell

Three to five randomly selected fields per well were photographed. Images were collected and pooled from two or three independent experiments. The purity of myogenic progenitors was determined by dividing the number of myogenic $marker^+$ cells by the number of $DAPI^+$ nuclei. To assess the efficiency of adipogenic differentiation, we quantified the number of adipocytes per field or Bodipy-stained area. $MyHC^+$ area per well was quantified to assess the efficiency of myogenic differentiation.

RNA Extraction and RT-PCR

Total RNA was extracted using an RNeasy Micro Kit (Qiagen), and equal amounts of RNA were reverse transcribed into cDNA using a QuantiTect Reverse Transcription Kit (Qiagen). Real-time qPCR was performed on a Thermal Cycler Dice Real Time System (Takara) or LightCycler 480 System (Roche). Specific primer sequences used in this study are described in Supplemental Experimental Procedures.

Statistics

The significance of differences among experimental groups was assessed by Student's t test or one-way ANOVA followed by Tukey's post hoc test.

SUPPLEMENTAL INFORMATION

Supplemental Information includes Supplemental Experimental Procedures, six figures, and one table and can be found with this article online at http://dx.doi.org/10.1016/j.stemcr.2016.07.004.

AUTHOR CONTRIBUTIONS

A.U. conceived the study. A.U. was responsible for designing and performing experiments, analyzing data, interpreting results, and writing the manuscript. M.N. helped with immunoblotting experiments. M.I.-U. and T.K. helped with immunofluorescent experiments. N.Y. helped with FACS experiments. M.M., A.Y., and H.Y. helped with experiments related to human tissues. S.M., A.N., Y.M.S., S.T., and S.F. performed experiments and analyzed data related to iPSCs. I.N. provided DMD samples. A.U. and K.T. coordinated the project.

ACKNOWLEDGMENTS

We thank K. Ono for proofreading the paper. This work was supported by AMED Research Center Network for Realization of Regenerative Medicine, AMED Health and Labor Sciences Research Grants for Comprehensive Research on Persons with Disabilities, Japan Foundation for Aging and Health, JSPS KAKENHI Grant Number 15K12675, Astellas Pharma, and the 24th General Assembly of the Japanese Association of Medical Sciences.

Received: June 3, 2016
Revised: July 8, 2016
Accepted: July 8, 2016
Published: August 9, 2016

REFERENCES

Agley, C.C., Rowlerson, A.M., Velloso, C.P., Lazarus, N.R., and Harridge, S.D. (2013). Human skeletal muscle fibroblasts, but not myogenic cells, readily undergo adipogenic differentiation. J. Cell Sci. *126*, 5610–5625.

Arrighi, N., Moratal, C., Clement, N., Giorgetti-Peraldi, S., Peraldi, P., Loubat, A., Kurzenne, J.Y., Dani, C., Chopard, A., and Dechesne, C.A. (2015). Characterization of adipocytes derived from fibro/adipogenic progenitors resident in human skeletal muscle. Cell Death Dis. *6*, e1733.

Balazs, A.B., Fabian, A.J., Esmon, C.T., and Mulligan, R.C. (2006). Endothelial protein C receptor (CD201) explicitly identifies hematopoietic stem cells in murine bone marrow. Blood *107*, 2317–2321.

Bischof, R. (2004). Satellite and stem cells in muscle regeneration. In Myology, A.G. Engel and C. Franzini-Armstrong, eds. (New York: McGraw-Hill), pp. 66–86.

Boldrin, L., and Morgan, J.E. (2012). Human satellite cells: identification on human muscle fibres. PLoS Curr. *3*, RRN1294.

Boldrin, L., Muntoni, F., and Morgan, J.E. (2010). Are human and mouse satellite cells really the same? J. Histochem. Cytochem. *58*, 941–955.

Buhring, H.J., Kuci, S., Conze, T., Rathke, G., Bartolovic, K., Grunebach, F., Scherl-Mostageer, M., Brummendorf, T.H., Schweifer, N., and Lammers, R. (2004). CDCP1 identifies a broad spectrum of normal and malignant stem/progenitor cell subsets of hematopoietic and nonhematopoietic origin. Stem Cells *22*, 334–343.

Cao, M., Gao, J., Zhou, H., Huang, J., You, A., Guo, Z., Fang, F., Zhang, W., Song, T., and Zhang, T. (2015). HIF-2alpha regulates CDCP1 to promote PKCdelta-mediated migration in hepatocellular carcinoma. Tumour Biol. *37*, 1651–1662.

Castiglioni, A., Hettmer, S., Lynes, M.D., Rao, T.N., Tchessalova, D., Sinha, I., Lee, B.T., Tseng, Y.H., and Wagers, A.J. (2014). Isolation of progenitors that exhibit myogenic/osteogenic bipotency in vitro by fluorescence-activated cell sorting from human fetal muscle. Stem Cell Rep. *2*, 92–106.

Charville, G.W., Cheung, T.H., Yoo, B., Santos, P.J., Lee, G.K., Shrager, J.B., and Rando, T.A. (2015). Ex vivo expansion and in vivo self-renewal of human muscle stem cells. Stem Cell Rep. *5*, 621–632.

Conze, T., Lammers, R., Kuci, S., Scherl-Mostageer, M., Schweifer, N., Kanz, L., and Buhring, H.J. (2003). CDCP1 is a novel marker for hematopoietic stem cells. Ann. N. Y Acad. Sci. *996*, 222–226.

Custer, M.C., Risinger, J.I., Hoover, S., Simpson, R.M., Patterson, T., and Barrett, J.C. (2006). Characterization of an antibody that can detect the Kai1/CD82 murine metastasis suppressor. Prostate *66*, 567–577.

Dong, J.T., Lamb, P.W., Rinker-Schaeffer, C.W., Vukanovic, J., Ichikawa, T., Isaacs, J.T., and Barrett, J.C. (1995). KAI1, a metastasis suppressor gene for prostate cancer on human chromosome 11p11.2. Science *268*, 884–886.

Downey, J., Lauzier, D., Kloen, P., Klarskov, K., Richter, M., Hamdy, R., Faucheux, N., Scime, A., Balg, F., and Grenier, G. (2015). Prospective heterotopic ossification progenitors in adult human skeletal muscle. Bone *71*, 164–170.

Emerling, B.M., Benes, C.H., Poulogiannis, G., Bell, E.L., Courtney, K., Liu, H., Choo-Wing, R., Bellinger, G., Tsukazawa, K.S., Brown, V., et al. (2013). Identification of CDCP1 as a hypoxia-inducible factor 2alpha (HIF-2alpha) target gene that is associated with survival in clear cell renal cell carcinoma patients. Proc. Natl. Acad. Sci. USA *110*, 3483–3488.

Fukada, S., Uezumi, A., Ikemoto, M., Masuda, S., Segawa, M., Tanimura, N., Yamamoto, H., Miyagoe-Suzuki, Y., and Takeda, S. (2007). Molecular signature of quiescent satellite cells in adult skeletal muscle. Stem Cells *25*, 2448–2459.

Gur-Cohen, S., Itkin, T., Chakrabarty, S., Graf, C., Kollet, O., Ludin, A., Golan, K., Kalinkovich, A., Ledergor, G., Wong, E., et al. (2015). PAR1 signaling regulates the retention and recruitment of EPCR-expressing bone marrow hematopoietic stem cells. Nat. Med. *21*, 1307–1317.

Hosoyama, T., McGivern, J.V., Van Dyke, J.M., Ebert, A.D., and Suzuki, M. (2014). Derivation of myogenic progenitors directly from human pluripotent stem cells using a sphere-based culture. Stem Cells Transl. Med. *3*, 564–574.

Huang, C., Taki, T., Adachi, M., Yagita, M., Sawada, S., Takabayashi, A., Inufusa, H., Yoshie, O., and Miyake, M. (1997). MRP-1/CD9 and KAI1/CD82 expression in normal and various cancer tissues. Int. J. Oncol. *11*, 1045–1051.

Hur, J., Choi, J.I., Lee, H., Nham, P., Kim, T.W., Chae, C.W., Yun, J.Y., Kang, J.A., Kang, J., Lee, S.E., et al. (2016). CD82/KAI1 maintains the dormancy of long-term hematopoietic stem cells through interaction with DARC-expressing macrophages. Cell Stem Cell *18*, 508–521.

Ikemoto, M., Fukada, S., Uezumi, A., Masuda, S., Miyoshi, H., Yamamoto, H., Wada, M.R., Masubuchi, N., Miyagoe-Suzuki, Y., and Takeda, S. (2007). Autologous transplantation of SM/C-2.6(+) satellite cells transduced with micro-dystrophin CS1 cDNA by lentiviral vector into mdx mice. Mol. Ther. *15*, 2178–2185.

Joe, A.W., Yi, L., Natarajan, A., Le Grand, F., So, L., Wang, J., Rudnicki, M.A., and Rossi, F.M. (2010). Muscle injury activates resident fibro/adipogenic progenitors that facilitate myogenesis. Nat. Cell Biol. *12*, 153–163.

Lecourt, S., Marolleau, J.P., Fromigue, O., Vauchez, K., Andriamanalijaona, R., Ternaux, B., Lacassagne, M.N., Robert, I., Boumediene, K., Chereau, F., et al. (2010). Characterization of distinct mesenchymal-like cell populations from human skeletal muscle in situ and in vitro. Exp. Cell Res. *316*, 2513–2526.

Liu, W.M., and Zhang, X.A. (2006). KAI1/CD82, a tumor metastasis suppressor. Cancer Lett. *240*, 183–194.

Mohan Rao, L.V., Esmon, C.T., and Pendurthi, U.R. (2014). Endothelial cell protein C receptor: a multiliganded and multifunctional receptor. Blood *124*, 1553–1562.

Nagira, M., Imai, T., Ishikawa, I., Uwabe, K.I., and Yoshie, O. (1994). Mouse homologue of C33 antigen (CD82), a member of

the transmembrane 4 superfamily: complementary DNA, genomic structure, and expression. Cell Immunol. *157*, 144–157.

Nakagawa, M., Koyanagi, M., Tanabe, K., Takahashi, K., Ichisaka, T., Aoi, T., Okita, K., Mochiduki, Y., Takizawa, N., and Yamanaka, S. (2008). Generation of induced pluripotent stem cells without Myc from mouse and human fibroblasts. Nat. Biotechnol. *26*, 101–106.

Okita, K., Matsumura, Y., Sato, Y., Okada, A., Morizane, A., Okamoto, S., Hong, H., Nakagawa, M., Tanabe, K., Tezuka, K., et al. (2011). A more efficient method to generate integration-free human iPS cells. Nat. Methods *8*, 409–412.

Peng, X.D., Xu, P.Z., Chen, M.L., Hahn-Windgassen, A., Skeen, J., Jacobs, J., Sundararajan, D., Chen, W.S., Crawford, S.E., Coleman, K.G., et al. (2003). Dwarfism, impaired skin development, skeletal muscle atrophy, delayed bone development, and impeded adipogenesis in mice lacking Akt1 and Akt2. Genes Dev. *17*, 1352–1365.

Pisani, D.F., Clement, N., Loubat, A., Plaisant, M., Sacconi, S., Kurzenne, J.Y., Desnuelle, C., Dani, C., and Dechesne, C.A. (2010a). Hierarchization of myogenic and adipogenic progenitors within human skeletal muscle. Stem Cells *28*, 2182–2194.

Pisani, D.F., Dechesne, C.A., Sacconi, S., Delplace, S., Belmonte, N., Cochet, O., Clement, N., Wdziekonski, B., Villageois, A.P., Butori, C., et al. (2010b). Isolation of a highly myogenic CD34-negative subset of human skeletal muscle cells free of adipogenic potential. Stem Cells *28*, 753–764.

Prusty, D., Park, B.H., Davis, K.E., and Farmer, S.R. (2002). Activation of MEK/ERK signaling promotes adipogenesis by enhancing peroxisome proliferator-activated receptor gamma (PPARgamma) and C/EBPalpha gene expression during the differentiation of 3T3-L1 preadipocytes. J. Biol. Chem. *277*, 46226–46232.

Razorenova, O.V., Finger, E.C., Colavitti, R., Chernikova, S.B., Boiko, A.D., Chan, C.K., Krieg, A., Bedogni, B., LaGory, E., Weissman, I.L., et al. (2011). VHL loss in renal cell carcinoma leads to up-regulation of CUB domain-containing protein 1 to stimulate PKCdelta-driven migration. Proc. Natl. Acad. Sci. USA *108*, 1931–1936.

Reimann, J., Brimah, K., Schroder, R., Wernig, A., Beauchamp, J.R., and Partridge, T.A. (2004). Pax7 distribution in human skeletal muscle biopsies and myogenic tissue cultures. Cell Tissue Res. *315*, 233–242.

Sajko, S., Kubinova, L., Cvetko, E., Kreft, M., Wernig, A., and Erzen, I. (2004). Frequency of M-cadherin-stained satellite cells declines in human muscles during aging. J. Histochem. Cytochem. *52*, 179–185.

Takahashi, K., Tanabe, K., Ohnuki, M., Narita, M., Ichisaka, T., Tomoda, K., and Yamanaka, S. (2007). Induction of pluripotent stem cells from adult human fibroblasts by defined factors. Cell *131*, 861–872.

Takeda, H., Fujimori, Y., Kai, S., Ogawa, H., and Nakano, T. (2010). CD318/CUB-domain-containing protein 1 expression on cord blood hematopoietic progenitors. Exp. Ther. Med. *1*, 497–501.

Uezumi, A., Fukada, S., Yamamoto, N., Takeda, S., and Tsuchida, K. (2010). Mesenchymal progenitors distinct from satellite cells contribute to ectopic fat cell formation in skeletal muscle. Nat. Cell Biol. *12*, 143–152.

Uezumi, A., Ito, T., Morikawa, D., Shimizu, N., Yoneda, T., Segawa, M., Yamaguchi, M., Ogawa, R., Matev, M.M., Miyagoe-Suzuki, Y., et al. (2011). Fibrosis and adipogenesis originate from a common mesenchymal progenitor in skeletal muscle. J. Cell Sci. *124*, 3654–3664.

Uezumi, A., Fukada, S., Yamamoto, N., Ikemoto-Uezumi, M., Nakatani, M., Morita, M., Yamaguchi, A., Yamada, H., Nishino, I., Hamada, Y., et al. (2014a). Identification and characterization of PDGFRalpha+ mesenchymal progenitors in human skeletal muscle. Cell Death Dis. *5*, e1186.

Uezumi, A., Ikemoto-Uezumi, M., and Tsuchida, K. (2014b). Roles of nonmyogenic mesenchymal progenitors in pathogenesis and regeneration of skeletal muscle. Front Physiol. *5*, 68.

Vauchez, K., Marolleau, J.P., Schmid, M., Khattar, P., Chapel, A., Catelain, C., Lecourt, S., Larghero, J., Fiszman, M., and Vilquin, J.T. (2009). Aldehyde dehydrogenase activity identifies a population of human skeletal muscle cells with high myogenic capacities. Mol. Ther. *17*, 1948–1958.

Wortmann, A., He, Y., Deryugina, E.I., Quigley, J.P., and Hooper, J.D. (2009). The cell surface glycoprotein CDCP1 in cancer—insights, opportunities, and challenges. IUBMB Life *61*, 723–730.

Wosczyna, M.N., Biswas, A.A., Cogswell, C.A., and Goldhamer, D.J. (2012). Multipotent progenitors resident in the skeletal muscle interstitium exhibit robust BMP-dependent osteogenic activity and mediate heterotopic ossification. J. Bone Miner Res. *27*, 1004–1017.

Xu, X., Wilschut, K.J., Kouklis, G., Tian, H., Hesse, R., Garland, C., Sbitany, H., Hansen, S., Seth, R., Knott, P.D., et al. (2015). Human satellite cell transplantation and regeneration from diverse skeletal muscles. Stem Cell Rep. *5*, 419–434.

Stem Cell Reports, Volume *7*

Supplemental Information

Cell-Surface Protein Profiling Identifies Distinctive Markers of Progenitor Cells in Human Skeletal Muscle

Akiyoshi Uezumi, Masashi Nakatani, Madoka Ikemoto-Uezumi, Naoki Yamamoto, Mitsuhiro Morita, Asami Yamaguchi, Harumoto Yamada, Takehiro Kasai, Satoru Masuda, Asako Narita, Yuko Miyagoe-Suzuki, Shin'ichi Takeda, So-ichiro Fukada, Ichizo Nishino, and Kunihiro Tsuchida

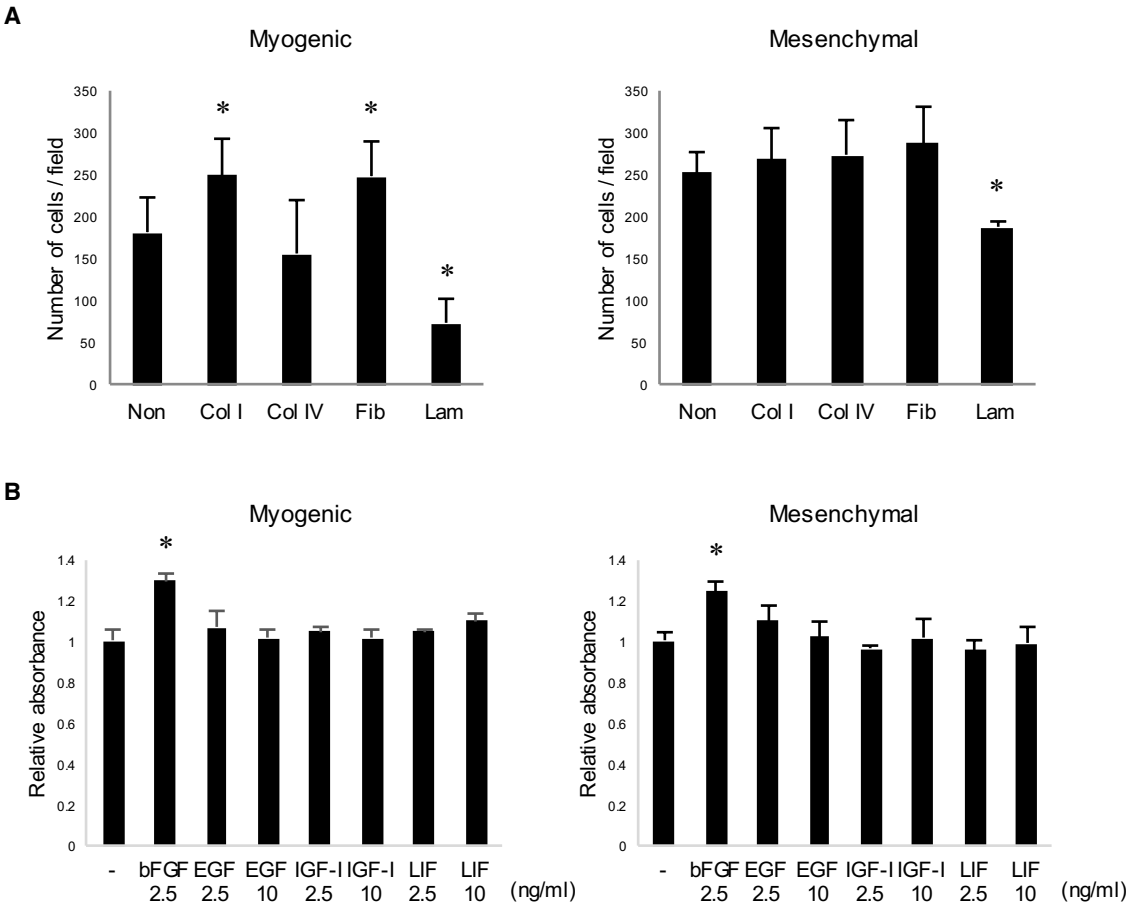
A
Myogenic
Mesenchymal
Number of cells / field
0
50
100
150
200
250
300
350
Non
Col I
Col IV
Fib
Lam
B
Relative absorbance
0
0.2
0.4
0.6
0.8
1
1.2
1.4
-
bFGF 2.5
EGF 2.5
EGF 10
IGF-I 2.5
IGF-I 10
LIF 2.5
LIF 10
(ng/ml)

Figure S1


0.0434 Blank
0.216 CD1a
0.111 CD1b
0.109 CD1c
0.0627 CD1d
0.109 CD2
0.0206 CD3
0.0445 CD4
0.0437 CD5
0.174 CD6
0.192 CD7
0.0878 CD8a
100 CD9
96.5 CD10
0.0222 CD11a
0.149 CD11b
0.196 CD11b (activated)
0.154 CD11c
100 CD13
0.155 CD14
0.0861 CD15
0.088 CD16
0.177 CD18
0.15 CD19
0.151 CD20
0.0222 CD21
0.13 CD22
0.0218 CD23
78 CD24
0.0438 CD25
80.1 CD26
0 CD27
0.592 CD28
100 CD29
0.044 CD30
0.238 CD31
0.0659 CD32
0.0872 CD33
0.0878 CD34
0.0444 CD35
0.132 CD36
0.0654 CD38
0.0658 CD39
0.438 CD40
0 CD41
0.0662 CD42b
0.274 CD43
99.9 CD44
0.0641 CD45
0.0216 CD45RA
0.0216 CD45RB
0.109 CD45RO
35.1 CD46
100 CD47
0.219 CD48
52.7 CD49a
100 CD49c
71.3 CD49d
100 CD49e
99.6 CD49f
0.0427 CD50 (ICAM-3)
99.9 CD51
93 CD51/61
0.044 CD52
0.111 CD53
3.04 CD54
75.6 CD55
97.4 CD56 (NCAM)
0.0641 CD57
99.8 CD58
100 CD59
29.3 CD61
0.0849 CD62E
0.106 CD62L
0.149 CD62P (P-selectin)
99.9 CD63
0.066 CD64
0.129 CD66a/c/e
0.133 CD66b
0.0432 CD69
0.388 CD70
95.9 CD71
100 CD73
0.172 CD74
0.577 CD79b
0.238 CD80
100 CD81
98.9 CD82
0.472 CD83
0.108 CD84
0.0214 CD85a (ILT5)
0.171 CD85d (ILT4)
0.107 CD85g (ILT7)
0.0852 CD85h (ILT1)
0.28 CD85j (ILT2)
0.0211 CD85k (ILT3)


0.11 Blank
0.11 CD86
0.107 CD87
0.238 CD88
0.0441 CD89
100 CD90 (Thy1)
0.133 CD93
0.264 CD94
99.5 CD95
0.11 CD96
63.4 CD97
100 CD99
0.0888 CD100
0 CD101 (BB27)
0.261 CD102
0.109 CD103
0 CD104
100 CD105
0.646 CD106
54.4 CD107a (LAMP-1)
97.9 CD108
91.4 CD109
31.9 CD111
99.4 CD112 (Nectin-2)
0.11 CD114
0.262 CD115
0.247 CD116
0.0658 CD117 (c-kit)
0.462 CD119 (IFN-γRα chain)
0.0441 CD122
0.132 CD123
0.223 CD124
0.086 CD126 (IL-6Rα)
0.0445 CD127 (IL-7Rα)
0.156 CD129 (IL-9R)
0.238 CD131
0.111 CD132
0.0672 CD134
0.0883 CD135
0.0877 CD137 (4-1BB)
0.176 CD137L (4-1BB L)
2.64 CD138
0.262 CD140a
0.554 CD140b
92.8 CD141
1.07 CD143
0.267 CD144
94.6 CD146
0.0895 CD148
0.156 CD150 (SLAM)
0.066 CD152
0.0667 CD154
98.1 CD155 (PVR)
97.8 CD156c (ADAM-10)
0.177 CD158a/h
0.0668 CD158b (NKAT2)
0.09 CD158d
0.0441 CD158e1 (NKB1)
0.169 CD158f
0.085 CD161
0.0849 CD162
0.108 CD163
93.9 CD164
99.2 CD165
98.8 CD166
0.26 CD167a (DDR1)
0.0649 CD169
0.197 CD170 (Siglec-5)
99.5 CD172a (SIRPα)
0.0433 CD172b (SIRPβ)
0.0856 CD172g (SIRPγ)
0.192 CD178 (Fas-L)
0.279 CD179a
0.108 CD179b
0.0648 CD180 (RP105)
0.172 CD181 (CXCR1)
0.0442 CD182 (CXCR2)
0.349 CD183
0.201 CD184 (CXCR4)
0.265 CD193 (CCR3)
0.712 CD195 (CCR5)
0.456 CD196
0.28 CD197 (CCR7)
0.149 CD200 (OX2)
0.191 CD200 R
53.5 CD201 (EPCR)
0.252 CD202b (Tie2/Tek)
0.213 CD203c (E-NPP3)
0.107 CD205 (DEC-205)
0.0214 CD206 (MMR)
0.107 CD207 (Langerin)
0.0429 CD209 (DC-SIGN)
0.243 CD210 (IL-10R)
39.6 CD213a2
0.432 CD215 (IL-15Rα)
0.235 CD218a (IL-18Rα)


0.0427 Blank
0.221 CD220
0.242 CD221 (IGF-1R)
0.0874 CD226 (DNAM-1)
0.0839 CD229 (Ly-9)
0.147 CD231 (TALLA)
0.129 CD235ab
0.176 CD243
0.0435 CD244 (2B4)
43.4 CD245 (p220/240)
0.568 CD252 (OX40L)
0.154 CD253 (Trail)
0.0667 CD254
0.153 CD255 (TWEAK)
0.683 CD257 (BAFF)
0.0653 CD258 (LIGHT)
0.0889 CD261 (DR4)
63.1 CD262 (DR5)
0.11 CD263 (DcR1)
29.3 CD266 (Fn14)
0.11 CD267 (TACI)
0.0221 CD268 (BAFF-R)
0.663 CD270 (HVEM)
78.2 CD271
20.4 CD273 (B7-DC)
94.6 CD274 (B7-H1)
0.109 CD275 (B7-H2)
100 CD276
0.789 CD277
0.0654 CD278 (ICOS)
0.0883 CD279 (PD-1)
0.281 CD282 (TLR2)
0.132 CD284 (TLR4)
0.044 CD286 (TLR6)
0.0219 CD290
0.087 CD294
100 CD298
0.109 CD300e (IREM-2)
0.153 CD300F
1.02 CD301
0.0222 CD303
88 CD304
0.0439 CD307
0.0888 CD307d (FcRL4)
0.0435 CD314 (NKG2D)
0.176 CD317
99.5 CD318 (CPCD1)
0.237 CD319 (CRACC)
0.0216 CD324 (E-Cadherin)
0.175 CD325
0.0861 CD326 (Ep-CAM)
0.0887 CD328 (Siglec-7)
0.13 CD334 (FGFR4)
0.022 CD335 (NKp46)
0.109 CD336 (NKp44)
0.0222 CD337 (NKp30)
0.0431 CD338 (ABCG2)
18.5 CD340 (erbB2)
24.5 CD344 (Frizzled-4)
0.0866 CD351
0.214 CD352 (NTB-A)
0.151 CD354 (TREM-1)
0.0659 CD355 (CRTAM)
0.239 CD357 (GITR)
8.96 CD360 (IL-21R)
100 β2-microglobulin
0.107 BTLA
0.308 C3AR
0.624 C5L2
0.308 CCR10
0.0646 CLEC12A
0.0879 CLEC9A
0.0428 CX3CR1
0.24 CXCR7
0.353 κ-Opioid Receptor
0 DLL1
0.0643 DLL4
0.0222 DR3 (TRAMP)
99.2 EGFR
0.262 erbB3/HER-3
0.066 FcεRIα
69.9 FcRL6
0.463 Galectin-9
8.8 GARP (LRRC32)
46 HLA-A,B,C
0.0853 HLA-A2
0.0215 HLA-DQ
0.149 HLA-DR
0.212 HLA-E
0.0638 HLA-G
0.35 IFN-γ R β chain
0 Ig light chain κ
0.0446 Ig light chain λ
0.169 IgD
0.0422 IgM
0.0844 IL-28RA

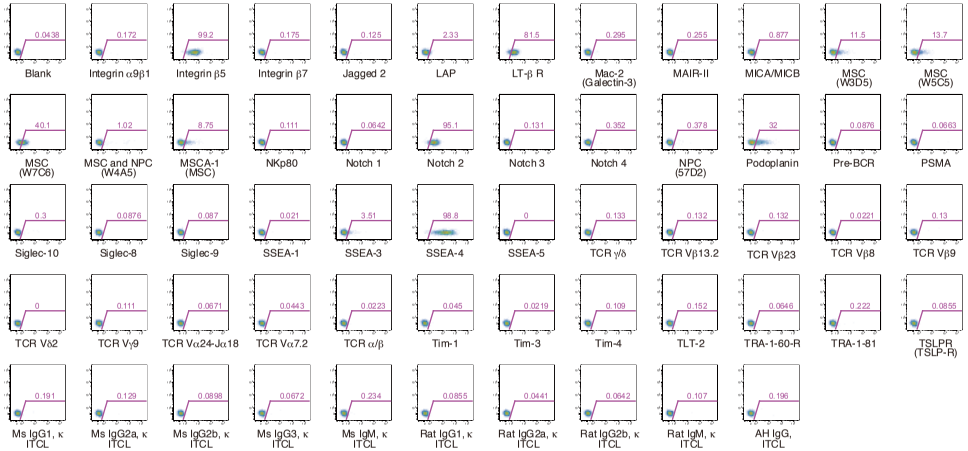
0.0438 Blank
0.172 Integrin α9β1
99.2 Integrin β5
0.175 Integrin β7
0.125 Jagged 2
2.33 LAP
81.5 LT-β R
0.295 Mac-2 (Galectin-3)
0.255 MAIR-II
0.877 MICA/MICB
11.5 MSC (W3D5)
13.7 MSC (W5C5)
40.1 MSC (W7C6)
1.02 MSC and NPC (W4A5)
8.75 MSCA-1 (MSC)
0.111 NKp80
0.0642 Notch 1
95.1 Notch 2
0.131 Notch 3
0.352 Notch 4
0.378 NPC (57D2)
32 Podoplanin
0.0876 Pre-BCR
0.0663 PSMA
0.3 Siglec-10
0.0876 Siglec-8
0.087 Siglec-9
0.021 SSEA-1
3.51 SSEA-3
98.8 SSEA-4
0 SSEA-5
0.133 TCR γ/δ
0.132 TCR Vβ13.2
0.132 TCR Vβ23
0.0221 TCR Vβ8
0.13 TCR Vβ9
0 TCR Vδ2
0.111 TCR Vγ9
0.0671 TCR Vα24-Jα18
0.0443 TCR Vα7.2
0.0223 TCR α/β
0.045 Tim-1
0.0219 Tim-3
0.109 Tim-4
0.152 TLT-2
0.0646 TRA-1-60-R
0.222 TRA-1-81
0.0855 TSLPR (TSLP-R)
0.191 Ms IgG1, κ ITCL
0.129 Ms IgG2a, κ ITCL
0.0898 Ms IgG2b, κ ITCL
0.0672 Ms IgG3, κ ITCL
0.234 Ms IgM, κ ITCL
0.0855 Rat IgG1, κ ITCL
0.0441 Rat IgG2a, κ ITCL
0.0642 Rat IgG2b, κ ITCL
0.107 Rat IgM, κ ITCL
0.196 AH IgG, ITCL

Figure S2


Blank
CD1a
CD1b
CD1c
CD1d
CD2
CD3
CD4
CD5
CD6
CD7
CD8a
CD9
CD10
CD11a
CD11b
CD11b (activated)
CD11c
CD13
CD14
CD15
CD16
CD18
CD19
CD20
CD21
CD22
CD23
CD24
CD25
CD26
CD27
CD28
CD29
CD30
CD31
CD32
CD33
CD34
CD35
CD36
CD38
CD39
CD40
CD41
CD42b
CD43
CD44
CD45
CD45RA
CD45RB
CD45RO
CD46
CD47
CD48
CD49a
CD49c
CD49d
CD49e
CD49f
CD50 (ICAM-3)
CD51
CD51/61
CD52
CD53
CD54
CD55
CD56 (NCAM)
CD57
CD58
CD59
CD61
CD62E
CD62L
CD62P (P-selectin)
CD63
CD64
CD66a/c/e
CD66b
CD69
CD70
CD71
CD73
CD74
CD79b
CD80
CD81
CD82
CD83
CD84
CD85a (ILT5)
CD85d (ILT4)
CD85g (ILT7)
CD85h (ILT1)
CD85j (ILT2)
CD85k (ILT3)


Blank
CD86
CD87
CD88
CD89
CD90 (Thy1)
CD93
CD94
CD95
CD96
CD97
CD99
CD100
CD101 (BB27)
CD102
CD103
CD104
CD105
CD106
CD107a (LAMP-1)
CD108
CD109
CD111
CD112 (Nectin-2)
CD114
CD115
CD116
CD117 (c-kit)
CD119 (IFN-γRα chain)
CD122
CD123
CD124
CD126 (IL-6Rα)
CD127 (IL-7Rα)
CD129 (IL-9R)
CD131
CD132
CD134
CD135
CD137 (4-1BB)
CD137L (4-1BB L)
CD138
CD140a
CD140b
CD141
CD143
CD144
CD146
CD148
CD150 (SLAM)
CD152
CD154
CD155 (PVR)
CD156c (ADAM-10)
CD158a/h
CD158b (NKAT2)
CD158d
CD158e1 (NKB1)
CD158f
CD161
CD162
CD163
CD164
CD165
CD166
CD167a (DDR1)
CD169
CD170 (Siglec-5)
CD172a (SIRPα)
CD172b (SIRPβ)
CD172g (SIRPγ)
CD178 (Fas-L)
CD179a
CD179b
CD180 (RP105)
CD181 (CXCR1)
CD182 (CXCR2)
CD183
CD184 (CXCR4)
CD193 (CCR3)
CD195 (CCR5)
CD196
CD197 (CCR7)
CD200 (OX2)
CD200 R
CD201 (EPCR)
CD202b (Tie2/Tek)
CD203c (E-NPP3)
CD205 (DEC-205)
CD206 (MMR)
CD207 (Langerin)
CD209 (DC-SIGN)
CD210 (IL-10R)
CD213a2
CD215 (IL-15Rα)
CD218a (IL-18Rα)


Blank
CD220
CD221 (IGF-1R)
CD226 (DNAM-1)
CD229 (Ly-9)
CD231 (TALLA)
CD235ab
CD243
CD244 (2B4)
CD245 (p220/240)
CD252 (OX40L)
CD253 (Trail)
CD254
CD255 (TWEAK)
CD257 (BAFF)
CD258 (LIGHT)
CD261 (DR4)
CD262 (DR5)
CD263 (DcR1)
CD266 (Fn14)
CD267 (TACI)
CD268 (BAFF-R)
CD270 (HVEM)
CD271
CD273 (B7-DC)
CD274 (B7-H1)
CD275 (B7-H2)
CD276
CD277
CD278 (ICOS)
CD279 (PD-1)
CD282 (TLR2)
CD284 (TLR4)
CD286 (TLR6)
CD290
CD294
CD298
CD300e (IREM-2)
CD300F
CD301
CD303
CD304
CD307
CD307d (FcRL4)
CD314 (NKG2D)
CD317
CD318 (CPCD1)
CD319 (CRACC)
CD324 (E-Cadherin)
CD325
CD326 (Ep-CAM)
CD328 (Siglec-7)
CD334 (FGFR4)
CD335 (NKp46)
CD336 (NKp44)
CD337 (NKp30)
CD338 (ABCG2)
CD340 (erbB2)
CD344 (Frizzled-4)
CD351
CD352 (NTB-A)
CD354 (TREM-1)
CD355 (CRTAM)
CD357 (GITR)
CD360 (IL-21R)
β2-microglobulin
BTLA
C3AR
C5L2
CCR10
CLEC12A
CLEC9A
CX3CR1
CXCR7
δ-Opioid Receptor
DLL1
DLL4
DR3 (TRAMP)
EGFR
erbB3/HER-3
FcεRIα
FcRL6
Galectin-9
GARP (LRRC32)
HLA-A,B,C
HLA-A2
HLA-DQ
HLA-DR
HLA-E
HLA-G
IFN-γ R β chain
Ig light chain κ
Ig light chain λ
IgD
IgM
IL-28RA

Blank
Integrin α9β1
Integrin β5
Integrin β7
Jagged 2
LAP
LT-β R
Mac-2 (Galectin-3)
MAIR-II
MICA/MICB
MSC (W3D5)
MSC (W5C5)
MSC (W7C6)
MSC and NPC (W4A5)
MSCA-1 (MSC)
NKp80
Notch 1
Notch 2
Notch 3
Notch 4
NPC (57D2)
Podoplanin
Pre-BCR
PSMA
Siglec-10
Siglec-8
Siglec-9
SSEA-1
SSEA-3
SSEA-4
SSEA-5
TCR γ/δ
TCR Vβ13.2
TCR Vβ8
TCR Vβ9
TCR Vδ2
TCR Vγ9
TCR Vα24-Jα18
TCR Vα7.2
TCR α/β
Tim-1
Tim-3
Tim-4
TLT-2
TRA-1-60-R
TRA-1-81
TSLPR (TSLP-R)
Ms IgG1, κ ITCL
Ms IgG2a, κ ITCL
Ms IgG2b, κ ITCL
Ms IgG3, κ ITCL
Ms IgM, κ ITCL
Rat IgG1, κ ITCL
Rat IgG2a, κ ITCL
Rat IgG2b, κ ITCL
Rat IgM, κ ITCL
AH IgG, ITCL

Figure S3

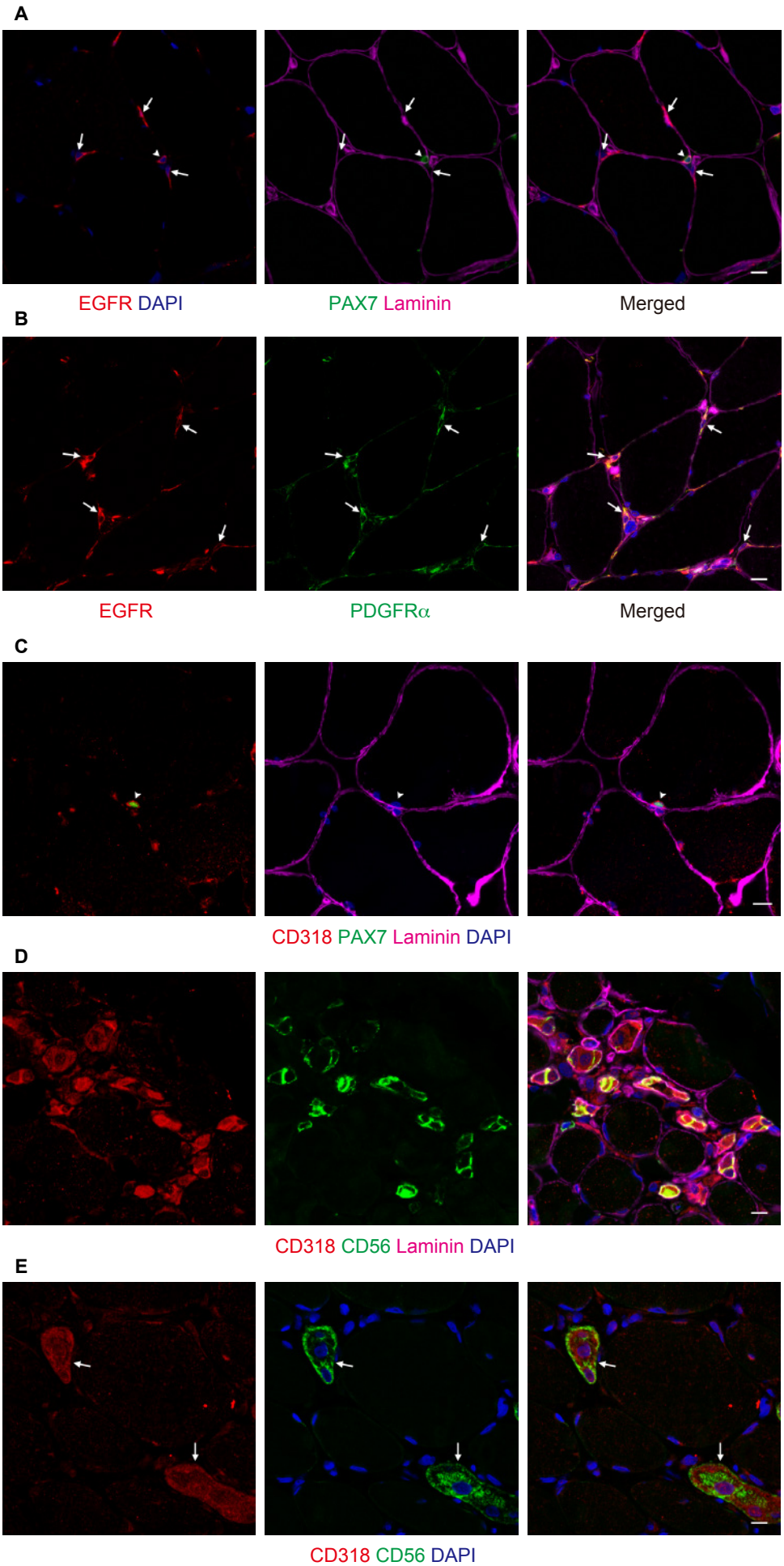
A
EGFR DAPI
PAX7 Laminin
Merged
B
EGFR
PDGFRα
Merged
C
CD318 PAX7 Laminin DAPI
D
CD318 CD56 Laminin DAPI
E
CD318 CD56 DAPI

Figure S4

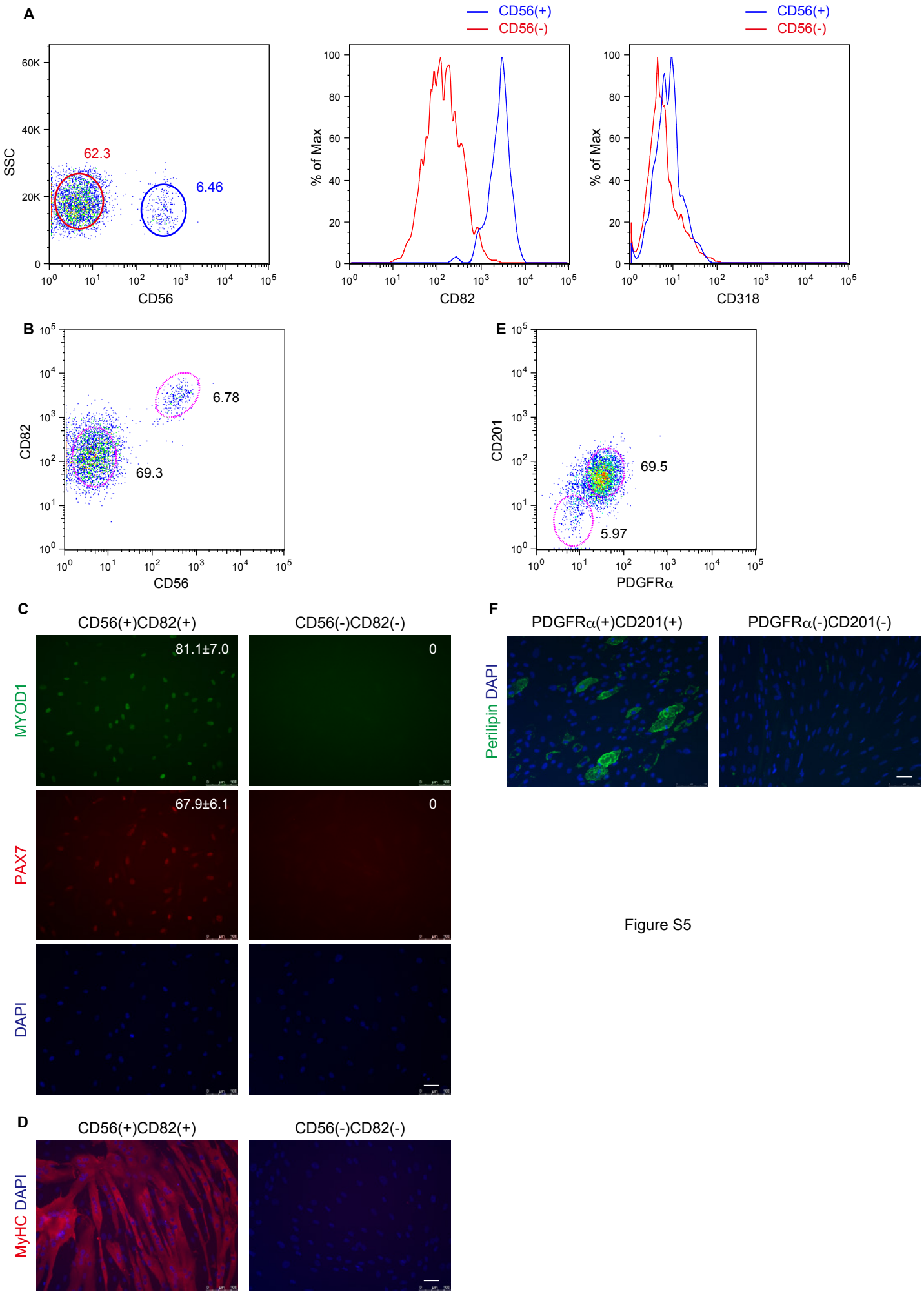
A
CD56(+)
CD56(-)
SSC
62.3
6.46
CD56
% of Max
CD82
CD318
B
CD82
6.78
69.3
CD56
E
CD201
69.5
5.97
PDGFRα
C
CD56(+)CD82(+)
CD56(-)CD82(-)
MYOD1
81.1±7.0
0
PAX7
67.9±6.1
0
DAPI
F
PDGFRα(+)CD201(+)
PDGFRα(-)CD201(-)
Perilipin DAPI
D
CD56(+)CD82(+)
CD56(-)CD82(-)
MyHC DAPI

Figure S5

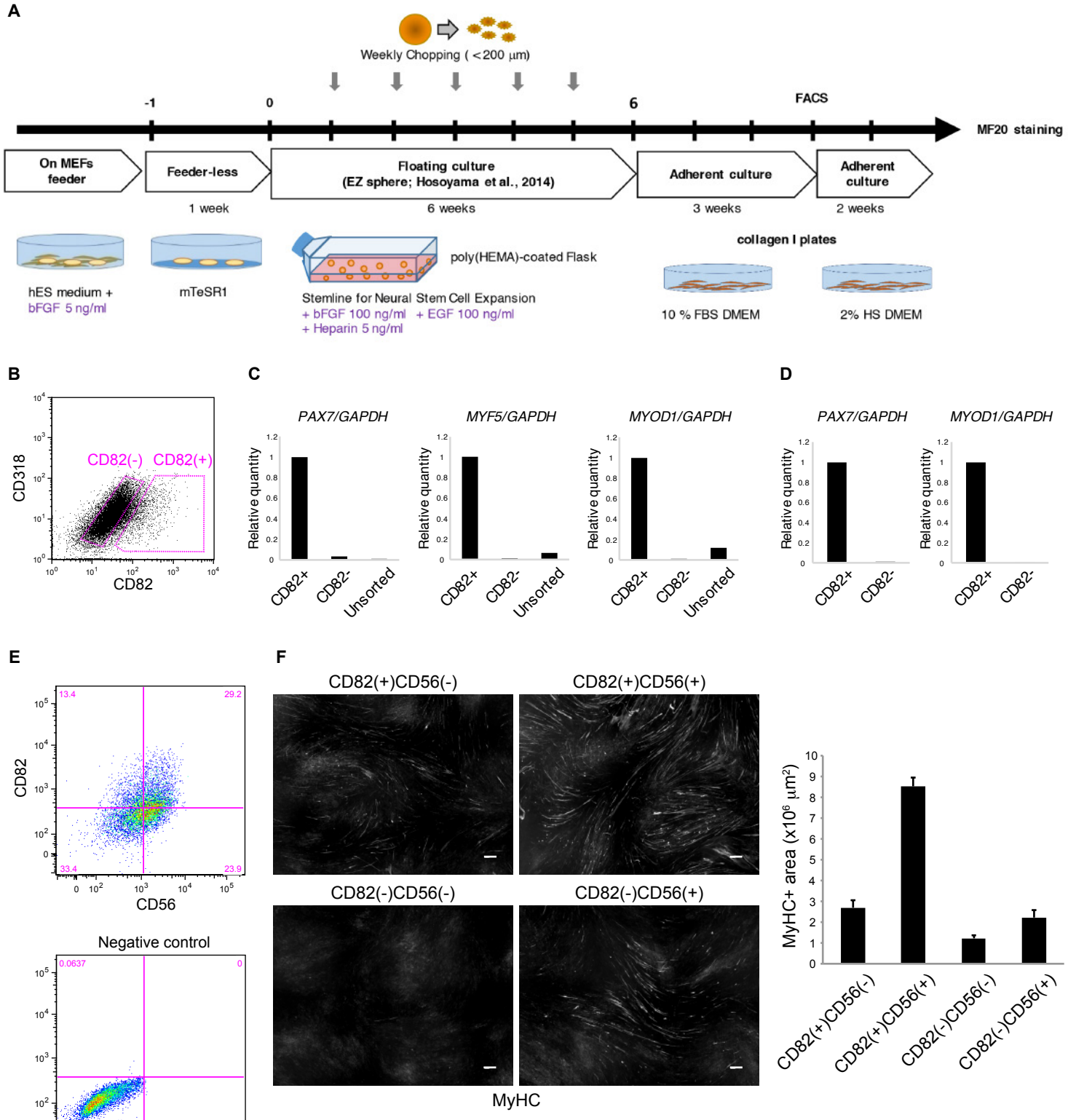
A
Weekly Chopping (<200 μm)
-1
0
6
FACS
MF20 staining
On MEFs feeder
Feeder-less
Floating culture (EZ sphere; Hosoyama et al., 2014)
Adherent culture
Adherent culture
1 week
6 weeks
3 weeks
2 weeks
hES medium + bFGF 5 ng/ml
mTeSR1
poly(HEMA)-coated Flask
Stemline for Neural Stem Cell Expansion
+ bFGF 100 ng/ml + EGF 100 ng/ml
+ Heparin 5 ng/ml
collagen I plates
10 % FBS DMEM
2% HS DMEM
B
CD82(-) CD82(+)
CD318
CD82
C
PAX7/GAPDH
MYF5/GAPDH
MYOD1/GAPDH
Relative quantity
CD82+
CD82-
Unsorted
D
PAX7/GAPDH
MYOD1/GAPDH
Relative quantity
CD82+
CD82-
E
CD82
CD56
13.4
29.2
33.4
23.9
Negative control
0.0637
0
99.8
0.102
F
CD82(+)CD56(-)
CD82(+)CD56(+)
CD82(-)CD56(-)
CD82(-)CD56(+)
MyHC
MyHC+ area (x10^6 μm^2)
CD82(+)CD56(-)
CD82(+)CD56(+)
CD82(-)CD56(-)
CD82(-)CD56(+)

Figure S6

Supplemental Figure Legends

Figure S1 (Related to Figure 1). Optimization of coating substrates and growth factors for the expansion of human muscle-derived progenitors.

(A) Muscle-derived progenitors were cultured for 3 d on the indicated coating substrates. Collagen I, collagen IV, fibronectin, and laminin were used as coating substrates. Number of cells per fields was quantified and expressed as means ± s.d., n=15 fields from three independent preparations. *P<0.01. (B) Muscle-derived progenitors were cultured for 3 d in medium containing indicated growth factors. Cell proliferation was measured by using WST-1 reagent and shown as means ± s.d. of three independent preparations. *P<0.01.

Figure S2 (Related to Figure 1). Entire data set of antibody array of cultured $CD56^+$ myogenic progenitors.

The entire FACS data of antibody array obtained from cultured $CD56^+$ myogenic progenitors were shown.

Figure S3 (Related to Figure 1). Entire data set of antibody array of cultured $PDGFR\alpha^+$ mesenchymal progenitors.

The entire FACS data of antibody array obtained from cultured $PDGFR\alpha^+$ mesenchymal progenitors were shown.

Figure S4 (Related to Figure 1 and 2). Expression of EGFR and CD318 in human skeletal muscle.

(A) Adult human muscle sections were stained with antibodies against EGFR, PAX7, and Laminin. Arrowheads indicate satellite cells located beneath the basement membrane. Arrows indicate $EGFR^+$ cells located in the interstitial space. (B) Adult human muscle sections were stained with antibodies against EGFR, PDGFRα, and Laminin. Arrows indicate $PDGFR\alpha^+EGFR^+$ cells located in the interstitial space. (C) Adult human muscle sections were stained with antibodies against CD318, PAX7, and Laminin. Arrowheads indicate satellite cells located beneath the basement membrane. (D) DMD muscle sections were stained with antibodies against CD318, CD56, and Laminin. (E) DMD muscle sections were stained

with antibodies against CD318 and CD56. Arrows indicate $CD56^+$ centrally-nucleated myofibers. Scale bars: 10 μm.

Figure S5 (Related to Figure 3). Purification of myogenic or mesenchymal progenitors from commercially available human myoblast culture.

(A) Cells in HSMM culture were stained with antibodies against CD56, CD82, and CD318. $CD56^+$ cells (blue) and $CD56^-$ negative cells (red) were analyzed for expression of CD82 and CD318 (shown in the right). (B) FACS sorting based on CD56 and CD82 expression. Sorting gates are shown in the panel. (C) The indicated cell populations were cultured in growth condition for 3 d, and then stained with antibodies against MYOD1 and PAX7. The percentages of positive cells are shown in the panels as means ± s.d., n=6 fields from two independent experiments. (D) The indicated cell populations were cultured in the myogenic differentiation condition for 5 d, and then stained with anti-MyHC antibody. (E) Cells in HSMM cultures were stained with anti-PDGFRα and anti-CD201 antibodies. Sorting gates are shown in the panel. (F) The indicated cell populations were subjected to the adipogenic condition and stained with anti-Perilipin antibody. Scale bars: 50 μm in C-F.

Figure S6 (Related to Figure 3). Isolation of myogenic progenitors from human iPSCs.

(A) Scheme of myogenic induction by the EZ sphere method from human iPSCs. (B) Clone 253G4 human iPSCs were induced to differentiate into a myogenic lineage and then maintained in DMEM supplemented with 2% HS. Induced cells were analyzed for CD82 and CD318 expression. (C) Expressions of myogenic progenitor genes in the indicated fractions of clone 253G4-derived cells. (D) Expressions of myogenic progenitor genes in the indicated fractions of clone 201B7-derived cells. (E) Clone 454E2 human iPS cells were induced to differentiate into the myogenic lineage and induced cells were analyzed for CD82 and CD56 expression. The lower plot shows negative control stained with isotype control antibodies. (F) Sorted fractions were cultured in DMEM supplemented with 2% HS for 2 wks and then subjected to immunofluorescent staining for MyHC. Scale bars: 250 μm. $MyHC^+$ area in each cell population was quantified and shown as means ± s.d.

Table S1. Cell surface genes that are up-regulated (> 5-fold) in quiescent satellite cells compared with non-myogenic cells, Related to Discussion

Genbank	Symbol	Description	Fold Change (vs non-myogenic)
NM_007588	Calcr	calcitonin receptor	83.7
NM_007662	Cdh15	cadherin 15	60.13
AW536432	Hs6st2	heparan sulfate 6-O-sulfotransferase 2	43.54
AB025413	Odz4	odd Oz/ten-m homolog 4 (Drosophila)	23.58
NM_008516	Lrrn1	leucine rich repeat protein 1, neuronal	21.4
NM_010298	Glrb	glycine receptor, beta subunit	20.46
NM_007656	Kai1	kangai 1 (suppression of tumorigenicity 6, prostate)	20.08
BB250384	Vcam1	BB250384 RIKEN full-length enriched, 7 days neonate cerebellum Mus musculus cDNA clone A730041B10 3' similar to M84487 Mouse vascular cell adhesion molecule-1 mRNA, mRNA sequence.	19.68
NM_007539	Bdkrb1	bradykinin receptor, beta 1	17.45
BC005679	Sdc4	syndecan 4	12.9
AF127140	Fgfr4	fibroblast growth factor receptor 4	9.342
AF311699	Chodl	chondrolectin	8.491
D87747	Cxcr4	chemokine (C-X-C motif) receptor 4	8.359
U37709	Musk	muscle, skeletal, receptor tyrosine kinase	8.045
M84756	Ank1	ankyrin 1, erythroid	7.864
AW494220	Mgl2	macrophage galactose N-acetyl-galactosamine specific lectin 2	7.444
AI849305	Ptprz1	protein tyrosine phosphatase, receptor type Z, polypeptide 1	7.268
NM_021301	Slc15a2	solute carrier family 15 (H+/peptide transporter), member 2	7.233
BC016109	AI481750	expressed sequence AI481750	7.225
BC015076	Eva	epithelial V-like antigen	6.968
AK010040	Il17r	interleukin 17 receptor	6.718
NM_053134	Pcdhb9	protocadherin beta 9	6.718
BB234940	Ddr1	discoidin domain receptor family, member 1	6.171
AK009873	2310047E01Rik	RIKEN cDNA 2310047E01 gene	6.075
BG094386	Dag1	dystroglycan 1	5.985
BQ173958	F2r	coagulation factor II (thrombin) receptor	5.966
NM_023450	2010204K13Rik	RIKEN cDNA 2010204K13 gene	5.927
X15052	Ncam1	neural cell adhesion molecule 1	5.477
AB026551	AA408868	expreexpressed sequence AA408868	5.41
NM_008398	Itga7	integrin alpha 7	5.254
NM_007429	Agtr2	angiotensin II receptor, type 2	5.096

Microarray data (Fukada et al., Stem Cells, 2007) is re-analyzed to identify cell surface genes that are specifically expressed in mouse satellite cells.

Supplemental Experimental procedures

Human muscle samples

Experiments using human samples were approved by the Ethical Review Board for Clinical Studies at Fujita Health University. Non-dystrophic muscle samples were obtained from gluteus medius muscles of 56 subjects ranging in age from 40 to 83 years undergoing total hip arthroplasty. DMD muscle samples were obtained from muscle (rectus femoris or biceps brachii) biopsies performed for diagnostic purposes on 11 DMD patients ranging in age from nine months to 23 years. Dystrophin deficiency was confirmed by immunohistochemistry and Western blotting. All patients or their parents gave written informed consent. A human myoblast culture was purchased from Lonza.

Dissociation of cells from muscle samples

Muscles were transferred to PBS. Nerves, blood vessels, tendons, and fat tissues were carefully removed. Trimmed muscles were minced and digested with 0.2% type II collagenase (Worthington) for 30 min at 37°C. Digested muscles were passed through an 18-gauge needle several times and further digested for 15 min at 37°C. Muscle slurries were filtered through a 100-μm cell strainer (BD Biosciences) and then through a 40-μm cell strainer (BD Biosciences). Erythrocytes were eliminated by treating the cells with Tris-buffered 0.8% NH_4Cl. Cells were resuspended in growth medium (GM) consisting of DMEM supplemented with 20% FBS, 1% penicillin-streptomycin, and 2.5 ng/ml bFGF (Katayama Chemical), seeded onto collagen I-coated dish (Iwaki), and maintained at 37°C in 5% CO_2 and 3% O_2.

FACS

Cells were trypsinized and resuspended in washing buffer consisting of PBS with 2.5% FBS, and stained with primary antibodies for 30 min at 4°C. Cells were then stained with streptavidin-PE/Cy5 (1:200, BD Pharmingen, #554062) or anti-Goat IgG-PE (1:200, R&D, #705-116-147) for 30 min at 4°C in the dark. Primary antibodies used for cell staining were VioBright FITC- or PE-conjugated anti-CD56 (1:20, Miltenyi Biotec, #130-104-944 or 130-090-755), FITC- or PE/Cy7-conjugated anti-CD56 (1:40, BD Pharmingen, #335791), biotinylated anti-PDGFRα (2.5 μg/ml, R&D, #BAF322), BB515-conjugated anti-PDGFRα (1:40, BD Pharmingen, #564594), PE- or Alexa Fluor 647-conjugated anti-CD82 (1:40,

BioLegend, #342104 or 342108), APC-conjugated anti-CD82 (1:200, Miltenyi Biotec, #130-101-311), PE-conjugated anti-CD274 (1:40, BioLegend, #329706), PE-conjugated anti-CD318 (1:40, BioLegend, #324006), PE-conjugated anti-CD201 (1:40, BioLegend, #351904), PE-conjugated anti-CD141 (1:40, BioLegend, #344104), and anti-PAR1 (5 μg/ml, R&D, #AF3855). Stained cells were analyzed by FACSVerse, FACSVantage SE (BD Biosciences), or MoFlo Astrios (Beckman Coulter). Cell sorting was performed on a FACSVantage SE or MoFlo Astrios.

Antibody screening

After cell sorting, $CD56^+$ cells or $PDGFR\alpha^+$ cells were cultured in GM on collagen I-coated dish at 37°C in 5% CO_2 and 3% O_2, and expanded to 1 x 10^8 cells. Antibody screening was carried out using a LEGENDScreen human cell screening kit (BioLegend). Expanded $CD56^+$ cells or $PDGFR\alpha^+$ cells were added to 96-well plates containing antibodies at 3 x 10^5 cells/well. Stained cells were analyzed by FACSVerse (BD Biosciences). Obtained data were further analyzed using FlowJo software (FlowJo LLC).

Cell culture

Sorted cells were cultured on Matrigel-coated (BD Biosciences) 48-well plates in GM at 37°C in 5% CO_2 and 3% O_2. Ten thousand cells were added per well. After 3 d incubation, cells were incubated in DMEM with 5% horse serum (HS) for 5 d at 37°C in 5% CO_2 and 21% O_2 for myogenic differentiation. For adipogenic differentiation, cells were treated with adipogenic induction medium consisting of DMEM with 10% FBS, 0.5 mM IBMX (Sigma), 0.25 μM dexamethasone (Sigma), and 10 μg/ml insulin (Sigma) for 3 d, followed by adipogenic maintenance medium consisting of DMEM with 10% FBS and 10 μg/ml insulin for 1 d at 37°C in 5% CO_2 and 21% O_2. This treatment was repeated three times. For knockdown of CD82, 5 nM of Silencer Select siRNA for CD82 (Ambion, sense: 5′-GCCCUCAAGGGUGUGUAUAtt-3′, antisense: 5′-UAUACACACCCUUGAGGGCag-3′) or control siRNA were transfected by using Lipofectamine RNAiMAX transfection reagent (Invitrogen). Five thousand cells were seeded per well of 96-well plate and cultured in GM for 3 d, and cell proliferation was measured by using Cell Counting Kit-8 (Dojindo). SB203580 (Wako), a p38 inhibitor, was used at

10 μM. APC (Haematologic Technologies) was used at 100 or 1000 nM. Human myoblast culture was maintained according to the manufacturer's instructions using a Clonetic SkGM-2 BulletKit (Lonza).

iPSCs and induction of myogenic progenitors

Human iPSCs (clone: 253G4 (Nakagawa et al., 2008), 201B7 (Takahashi et al., 2007), and 454E2 (Okita et al., 2011)) were provided by the Center for iPS Cell Research and Application. Myogenic cells were induced from iPSCs by the EZ sphere method as previously described (Hosoyama et al., 2014). Induced cells were trypsinized and resuspended in washing buffer, then subjected to FACS sorting. Sorted cells were subjected to RNA extraction or cultured on collagen-coated 24-well plates in DMEM supplemented with 10% FBS at 37°C in 5% CO_2. Myotube formation was induced by changing the medium to DMEM supplemented with 2% HS.

Generation of lentiviral vector and in vitro transduction

Plasmids required for generation of lentiviral vector were obtained from RIKEN BRC. The lentiviral vector was generated as described (Ikemoto et al., 2007). Sorted $CD201^+$ cells were plated on Matrigel-coated 24-well plates and cultured in GM containing 200 MOI of viral vector for overnight at 37°C in 5% CO_2 and 3% O_2. Infected cells were trypsinized and expanded in 60-mm dishes. When cells reached 80% confluency, cells were trypsinized and subjected to FACS sorting.

Transplantation experiment

Immunodeficient NOD/scid or NSG mice were used. All procedures using experimental animals were approved by the Institutional Animal Care and Use Committee at Fujita Health University. One day prior to transplantation, tibialis anterior (TA) muscles were injured with CTX or glycerol as described (Uezumi et al., 2010). Immediately after cell sorting, cells were resuspended in 25 μl PBS and transplanted into the TA muscles. Fifteen days after transplantation, TA muscles were excised and rapidly frozen in isopentane cooled with liquid nitrogen. For detection of $Venus^+$ cells, transplanted TA muscle were fixed with 4% PFA. Transplanted muscles were sectioned at 250 μm intervals from the proximal end to the mid-belly.

The maximal number of human Lamin A/C$^+$ cells, human Spectrin$^+$ myofibers, and human Lamin A/C$^+$PAX7$^+$ sublaminar satellite cells were recorded.

Histochemistry, cytochemistry, and microscopy

Muscle samples for histochemistry were rapidly frozen in isopentane cooled with liquid nitrogen. For CD82 and Spectrin immunostaining, frozen muscle sections were fixed with acetone at -20°C for 5 min. In other cases, sections were fixed with 4% PFA for 5 min. For CD82 and CD318 immunostaining, specimens were treated with Antigen Retrieval Reagent-Universal solution (R&D) at 95°C for 5 min. Cultured cells were rinsed with PBS and then fixed with 4% PFA for 5 min. Specimens were blocked with protein-block serum-free reagent (DAKO) for 15 min, and incubated with primary antibodies at 4°C overnight, followed by secondary staining. Primary antibodies used were anti-CD82 (1:50, Sigma, #HPA028900), anti-CD318 (1:100, Acris, #AP15947PU-N), anti-CD201 (2.5 μg/ml, R&D, #AF2245), anti-PDGFRα (2.5 μg/ml, R&D, #AF-307-NA), anti-M-cadherin (4 μg/ml, R&D, #AF4096), anti-PAX7 (1:2, DSHB), anti-CD56 (1:20, Miltenyi Biotec, #130-090-955), anti-Laminin (1:200, Sigma, #L9393), anti-Laminin (1:100, LSBio, #LS-C96142), anti-Collagen I (1:250, Abcam, #ab138492), anti-EGFR (1:200, Abcam, #ab52894), anti-MYOD1 (1:300, Abcam, #ab133627), anti-MYOG (1:300, Abcam, #ab124800), anti-MyHC (1:2, DSHB), anti-Sarcomeric α-actinin (1:200, Abcam, #ab68167), anti-Perilipin (1:250, Sigma, #P1873), anti-C/EBPα (1:400, Santa Cruz, #sc-9314), anti-PPARγ (1:100, Santa Cruz, #sc-7273), anti-GFP (1:200, Acris, #AB0020), anti-Ki67 (1:200, eBioscience, #51-5698-82), anti-human Lamin A/C (1:400, Epitomics, #2966-1), anti-human Spectrin (1:100, Leica, #NCL-SPEC1), and anti-Laminin α2 (1:400, Santa Cruz, #sc-59854). Secondary antibodies used with a dilution of 1:1000 were Alexa Fluor 488- or 647-conjugated anti-rabbit IgG (Molecular Probes, #A21206 or A31573), Cy3-conjugated anti-rabbit IgG (Jackson, #711-165-152), Alexa Fluor 488- or Cy3-conjugated anti-mouse IgG (Jackson, #715-545-150 or 715-165-150), Alexa Fluor 568-conjugated anti-mouse IgG (Molecular Probes, #A10037), Alexa Fluor 488-conjugated anti-goat IgG (Molecular Probes, #A11055), Cy3-conjugated anti-goat IgG (Jackson, #705-165-147), CF488A-conjugated anti-sheep IgG (Biotium, #20024), Alexa Fluor 647-conjugated anti-chick IgG (Jackson, #703-605-155), and Alexa Fluor 647-conjugated anti-rat IgG (Molecular Probes, #A21472). Specimens were counterstained with DAPI

(Invitrogen) and mounted with SlowFade Gold anti-fade reagent (Invitrogen). For sequential immunohistochemistry and HE staining, immunofluorescent staining was performed first and immunofluorescent images were captured. Slides were immersed in PBS to remove the cover glass and stained with HE. Then images of the corresponding HE-stained fields were captured. Stained cells and tissues were photographed using a fluorescence microscope BX51 (Olympus) equipped with a DP70 CCD camera (Olympus), an inverted fluorescence microscope BZ-9000 (Keyence), or an inverted fluorescence microscope DMI4000B (Leica) equipped with a DFC350FX CCD camera (Leica). Confocal images of muscle sections were taken using the confocal laser scanning microscope system LSM700 (Carl Zeiss).

Immunoblotting

Cells were lysed in lysis buffer consisting of 50 mM Tris-HCl (pH 7.5), 150 mM NaCl, 1 mM NaF, 1% NP-40, 1% sodium deoxycholate, 0.1% SDS, and protease inhibitor cocktail (Roche). For the detection of phosphorylated proteins, lysis buffer was supplemented with phosphatase inhibitor cocktail (Roche). Cell lysates were centrifuged at 1000 g for 10 min at 4°C and the supernatants were recovered. Aliquots of the lysates containing 10 μg of protein were separated by SDS-PAGE and transferred onto polyvinylidene difluoride membranes. The membranes were probed with anti-MYOD1 (1:1000, Abcam, #ab133627), anti-MYOG (1:1000, Abcam, #ab124800), anti-GAPDH (1:2000, Cell Signaling, #2118), anti-phospho-p38 (1:1000, Cell Signaling, #4511), anti-p38 (1:1000, Cell Signaling, #9212), anti-phospho-Akt (1:2000, Cell Signaling, #4060), anti-Akt (1:1000, Cell Signaling, #4691), anti-phospho-p44/42 MAPK (1:2000, Cell Signaling, #4370), and anti-p44/42 MAPK (1:1000, Cell Signaling, #9102). After incubation with horseradish peroxidase-conjugated secondary antibodies and chemiluminescence reactions, images of the developed immunoblots were captured using a Light-Capture imaging system (ATTO).

Quantitative analyses of cultured cell

Three to five randomly selected fields per well were photographed. Images were collected and pooled from two or three independent experiments. The purity of myogenic progenitors was determined by dividing the number of myogenic marker$^+$ cells by the number of DAPI$^+$ nuclei using Win ROOF

software (Mitani Corp). To assess the efficiency of adipogenic differentiation, number of perilipin^{+} adipocytes per field was counted, or adipocytes were stained by using Adipocyte Fluorescent Staining kit (Cosmo Bio) and Bodipy-stained area was measured by using ArrayScan XTI-HCS (ThermoFisher). To assess the efficiency of myogenic differentiation, four randomly selected fields were photographed per well. Images were collected and pooled from four to six independent wells. The MyHC^{+} area per well was measured by using BZ-X Analyzer software (Keyence).

RNA extraction and RT-PCR

Total RNA was extracted using an RNeasy Micro Kit (Qiagen), and equal amounts of RNA were reverse transcribed into cDNA using a QuantiTect Reverse Transcription Kit (Qiagen). Real-time quantitative PCR was performed on a Thermal Cycler Dice Real Time System (Takara) or LightCycler 480 System (Roche) under the following cycling conditions: 95°C for 10 sec, followed by 40 cycles of amplification (95°C for 5 sec, 60°C for 15 sec, 72°C for 10 sec). Specific primer sequences used in this study were 5′-GCTCATTCGAGACTACAACAGCA-3′ and 5′-CTTGACTTCGCAGGAACAGG-3′ for *CD82*, 5′-GACCCCTGCCTAACCACATC-3′ and 5′-GTCTCCTGGTAGCGGCAAAG-3′ for *PAX7*, 5′-GAGGTGTACCACGACCAACC-3′ and 5′-CCTGCTCTCTCAGCAACTCC-3′ for *MYF5*, 5′-GCCACAACGGACGACTTCTATG-3′ and 5′-TGCTCTTCGGGTTTCAGGAG-3′ for *MYOD1*, 5′-ATCATCTGCTCACGGCTGAC-3′ and 5′-GGGAAGGCCACAGACACATC-3′ for *MYOG*, 5′-CGTCAAAGGTGAAGCAGGAC-3′ and 5′-CTCCAGTGCCCGTAGATCAG-3′ for *NDUFA13*, and 5′-ACCCACTCCTCCACCTTTGA-3′ and 5′-TTGCTGTAGCCAAATTCGTTG-3′ for *GAPDH*. The following primers were used for generating standard samples: 5′-GGGTCTTCATCAATGGGCGA-3′ and 5′-GTCACAGTGCCCATCCTTCA-3′ for *PAX7*, 5′-TCAGCAGGATGGACGTGA-3′ and 5′-GGAGGTGATCCGGTCCACTA-3′ for *MYF5*, 5′-GAAAGTTCCGGCCACTCTCT-3′and 5′-CTGGTTTGGATTGCTCGACG-3′ for *MYOD1*, 5′-CCATCACCATCTTCCAGGAG-3′ and 5′-CCTGCTTCACCACCTTCTTG-3′ for *GAPDH*.

Statistics

The significance of differences among experimental groups was assessed by Student's t-test or one-way analysis of variance (ANOVA) followed by Tukey's post-hoc test.